Flavor SU(3) symmetry and QCD factorization in $B \to PP$ and PV decays

Hai-Yang Cheng* and Sechul Oh†

Institute of Physics, Academia Sinica, Taipei 115, Taiwan

(Dated: January 20, 2013)

Abstract

Using flavor SU(3) symmetry, we perform a model-independent analysis of charmless $\bar{B}_{u,d}(\bar{B}_s) \to PP$, PV decays. All the relevant topological diagrams, including the presumably subleading diagrams, such as the QCD- and EW-penguin exchange diagrams and flavor-singlet weak annihilation ones, are introduced. Indeed, the QCD-penguin exchange diagram turns out to be important in understanding the data for penguin-dominated decay modes. In this work we make efforts to bridge the (model-independent but less quantitative) topological diagram or flavor SU(3) approach and the (quantitative but somewhat model-dependent) QCD factorization (QCDF) approach in these decays, by explicitly showing how to translate each flavor SU(3) amplitude into the corresponding terms in the QCDF framework. After estimating each flavor SU(3) amplitude numerically using QCDF, we discuss various physical consequences, including SU(3) breaking effects and some useful SU(3) relations among decay amplitudes of $\bar{B}_s \to PV$ and $\bar{B}_d \to PV$.

* Email: phcheng@phys.sinica.edu.tw
† Email: scoh@phys.sinica.edu.tw

I. INTRODUCTION

A large number of hadronic $B_{u,d}$ decay events have been collected at the B factories which enable us to make accurate measurements of branching fractions (BFs) and direct CP asymmetries for many modes. With the advent of the LHCb experiment, a tremendous amount of new experimental data on B decays is expected to be obtained. In particular, various decay processes of heavier B_s and B_c mesons as well as very rare B decay modes are expected to be observed.

In earlier works on hadronic decays of B mesons, the factorization hypothesis, based on the color transparency argument, was usually assumed to estimate the hadronic matrix elements which are inevitably involved in theoretical calculations of the decay amplitudes for these processes. Under the factorization assumption, the matrix element of a four-quark operator is expressed as a product of a decay constant and a form factor. Naive factorization is simple but fails to describe color-suppressed modes. This is ascribed to the fact that color-suppressed decays receive sizable nonfactorizable contributions that have been neglected in naive factorization. Another issue is that the decay amplitude under naive factorization is not truly physical because the renormalization scale and scheme dependence of the Wilson coefficients $c_i(\mu)$ are not compensated by that of the matrix element $\langle M_1 M_2|O_i|B\rangle(\mu)$. In the improved "generalized factorization" approach [1, 2], nonfactorizable effects are absorbed into the parameter $N_c^{\rm eff}$, the effective number of colors. This parameter can be empirically determined from experiment.

With the advent of heavy quark effective theory, nonleptonic B decays can be analyzed systematically within the QCD framework. There are three popular approaches available in this regard: QCD factorization (QCDF) [3], perturbative QCD (pQCD) [4] and soft-collinear effective theory (SCET) [5]. In QCDF and SCET, power corrections of order $\Lambda_{\rm QCD}/m_b$ are often plagued by the end-point divergence that in turn breaks the factorization theorem. As a consequence, the estimate of power corrections is generally model dependent and can only be studied in a phenomenological way. In the pQCD approach, the endpoint singularity is cured by including the parton's transverse momentum.

Because a reliable evaluation of hadronic matrix elements is very difficult in general, an alternative approach which is essentially model independent is based on the diagrammatic approach [6–8]. In this approach, the topological diagrams are classified according to the

topologies of weak interactions with all strong interaction effects included. Based on flavor SU(3) symmetry, this model-independent analysis enables us to extract the topological amplitudes and sense the relative importance of different underlying decay mechanisms. When enough measurements are made with sufficient accuracy, we can extract the diagrammatic amplitudes from experiment and compare to theoretical estimates, especially checking whether there are any significant final-state interactions or whether the weak annihilation diagrams can be ignored as often asserted in the literature. The diagrammatic approach was applied to hadronic B decays first in [9]. Various topological amplitudes have been extracted from the data in [10–13] after making some reasonable approximations.

Based on SU(3) flavor symmetry, the decay amplitudes also can be decomposed into linear combinations of the $\mathrm{SU(3)_F}$ amplitudes which are SU(3) reduced matrix elements [14–17]. This approach is equivalent to the diagrammatic approach when SU(3) flavor symmetry is imposed to the latter.

In this work we make efforts to bridge these two different approaches, using QCDF and flavor SU(3) symmetry, in $\bar{B}_{u,d}(\bar{B}_s) \to PP,\ PV$ decays. For this aim, we first introduce all the relevant topological diagrams, including the presumably subleading diagrams, such as the QCD- and EW-penguin exchange ones and flavor-singlet weak annihilation ones, some of which turn out to be important especially in penguin-dominant decay processes. Then all these decay modes are analyzed by using the *intuitive* topological diagrams and expressed in terms of the $\mathrm{SU(3)_F}$ amplitudes. Each $\mathrm{SU(3)_F}$ amplitude is *translated into* the corresponding terms in the framework of QCDF. Applying these relations, one can easily find the rather *sophisticated* results of the relevant decay amplitudes calculated in the QCDF framework. The magnitude and the strong phase of each $\mathrm{SU(3)_F}$ amplitude are numerically estimated in QCDF. We further discuss some examples of the applications, including the effects of $\mathrm{SU(3)_F}$ breaking and useful $\mathrm{SU(3)_F}$ relations among decay amplitudes.

This paper is organized as follows. In Sec. II, we introduce topological quark diagrams relevant to $\bar{B}_{u,d}(\bar{B}_s) \to PP,\ PV$ decays and the framework of QCDF. The explicit $\mathrm{SU(3)_F}$ decomposition of the decay amplitudes and the relations between the $\mathrm{SU(3)_F}$ amplitudes and the QCDF terms are presented. In Sec. III, we make a numerical estimation of the $\mathrm{SU(3)_F}$ amplitudes and discuss its consequences and some applications. Our conclusions are given in Sec. IV.

II. FLAVOR SU(3) ANALYSIS AND QCD FACTORIZATION

It has been established sometime ago that a least model-dependent analysis of heavy meson decays can be carried out in the so-called quark-diagram approach. [1] In this diagrammatic scenario, all two-body nonleptonic weak decays of heavy mesons can be expressed in terms of six distinct quark diagrams [6–8]: [2] T, the color-allowed external W-emission tree diagram; C, the color-suppressed internal W-emission diagram; E, the W-exchange diagram; A, the W-annihilation diagram; P, the horizontal W-loop diagram; and V, the vertical W-loop diagram. (The one-gluon exchange approximation of the P graph is the so-called "penguin diagram".) For the analysis of charmless B decays, one adds the variants of the penguin diagram such as the electroweak penguin and the penguin annihilation and singlet penguins, as will be discussed below. It should be stressed that these diagrams are classified according to the topologies of weak interactions with all strong interaction effects encoded, and hence they are *not* Feynman graphs. All quark graphs used in this approach are topological and meant to have all the strong interactions included, *i.e.*, gluon lines are included implicitly in all possible ways. Therefore, analyses of topological graphs can provide information on final-state interactions (FSIs).

In $\mathrm{SU(3)_F}$ decomposition of the decay amplitudes for $\bar{B}_{u,d}(\bar{B}_s) \to M_1 M_2$ (with $M_1 M_2 = P_1 P_2,\ PV,\ VP$) modes [15], we represent the decay amplitudes in terms of topological quark diagram contributions. The topological amplitudes which will be referred to as $\mathrm{SU(3)_F}$ amplitudes hereafter, corresponding to different topological quark diagrams, as shown in Figs. 1-3, can be classified into three distinct groups as follows:

(i) *Tree and penguin amplitudes*

T : color-favored tree amplitude (equivalently, external W-emission),

C : color-suppressed tree amplitude (equivalently, internal W-emission),

P : QCD-penguin amplitude,

S : singlet QCD-penguin amplitude involving $\mathrm{SU(3)_F}$-*singlet* mesons (e.g., $\eta^{(\prime)},\ \omega,\ \phi$),

$P_{\rm EW}$: color-favored EW-penguin amplitude,

$P_{\rm EW}^C$: color-suppressed EW-penguin amplitude,

[1] It is also referred to as the flavor-flow diagram or topological-diagram approach in the literature.

[2] Historically, the quark-graph amplitudes T, C, E, A, P named in [15] were originally denoted by A, B, C, D, E, respectively, in [7, 8].

(ii) *Weak annihilation amplitudes*

E : W-exchange amplitude,

A : W-annihilation amplitude,

(E and A are often jointly called "weak annihilation".)

PE : QCD-penguin exchange amplitude,

PA : QCD-penguin annihilation amplitude,

$PE_{\rm EW}$: EW-penguin exchange amplitude,

$PA_{\rm EW}$: EW-penguin annihilation amplitude,

(PE and PA are also jointly called "weak penguin annihilation".)

(iii) *Flavor-singlet weak annihilation amplitudes*: all involving $\mathrm{SU(3)_F}$-*singlet* mesons [3]

SE : singlet W-exchange amplitude,

SA : singlet W-annihilation amplitude,

SPE : singlet QCD-penguin exchange amplitude,

SPA : singlet QCD-penguin annihilation amplitude,

$SPE_{\rm EW}$: singlet EW-penguin exchange amplitude,

$SPA_{\rm EW}$: singlet EW-penguin annihilation amplitude.

Within the framework of QCD factorization [20], the effective Hamiltonian matrix elements for $\bar{B} \to M_1 M_2$ ($M_1 M_2 = P_1 P_2, PV$) are written in the form

$$\langle M_1 M_2 | \mathcal{H}_{\rm eff} | \bar{B} \rangle = \frac{G_F}{\sqrt{2}} \sum_{p=u,c} \lambda_p^r \, \langle M_1 M_2 | \mathcal{T}_{\mathcal{A}}{}^p + \mathcal{T}_{\mathcal{B}}{}^p | \bar{B} \rangle \ , \tag{1}$$

where the Cabibbo-Kobayashi-Maskawa (CKM) factor $\lambda_p^r \equiv V_{pb} V_{pr}^*$ with $r = s, d$. $\mathcal{T}_{\mathcal{A}}{}^p$ describes contributions from naive factorization, vertex corrections, penguin contractions and spectator scattering expressed in terms of the flavor operators a_i^p, while $\mathcal{T}_{\mathcal{B}}{}^p$ contains annihilation topology amplitudes characterized by the annihilation operators b_j^p. The flavor operators a_i^p are basically the Wilson coefficients in conjunction with short-distance nonfactorizable corrections such as vertex corrections and hard spectator interactions. In general, they have the expressions [20, 21]

$$a_i^p(M_1 M_2) = \left(c_i + \frac{c_{i\pm1}}{N_c} \right) N_i(M_2) + \frac{c_{i\pm1}}{N_c} \, \frac{C_F \alpha_s}{4\pi} \Big[V_i(M_2) + \frac{4\pi^2}{N_c} H_i(M_1 M_2) \Big] + P_i^p(M_2) \ , \tag{2}$$

[3] The singlet amplitudes SE and SA were first discussed in [18, 19] as the disconnected hairpin amplitudes and denoted by E_h and A_h, respectively, in [19].

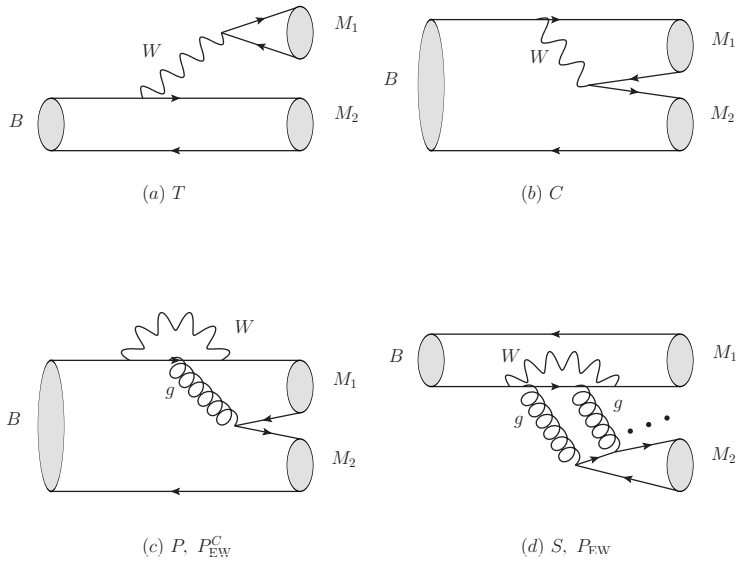

FIG. 1: Topology of possible diagrams: (a) Color-allowed tree [T], (b) Color-suppressed tree [C], (c) QCD-penguin [P], (d) Singlet QCD-penguin [S] diagrams with 2 (3) gluon lines for M_2 being a pseudoscalar meson P (a vector meson V). The color-suppressed EW-penguin [$P_{\rm EW}^C$] and color-favored EW-penguin [$P_{\rm EW}$] diagrams are obtained by replacing the gluon line from (c) and all the gluon lines from (d), respectively, by a single Z-boson or photon line.

where $i = 1, \cdots, 10$, the upper (lower) signs apply when i is odd (even), c_i are the Wilson coefficients, $C_F = (N_c^2 - 1)/(2N_c)$ with $N_c = 3$, M_2 is the emitted meson and M_1 shares the same spectator quark with the B meson. The quantities $N_i(M_2) = 0$ or 1 for $i = 6, 8$ and $M_2 = V$ or else, respectively. The quantities $V_i(M_2)$ account for vertex corrections, $H_i(M_1 M_2)$ for hard spectator interactions with a hard gluon exchange between the emitted meson and the spectator quark of the B meson and $P_i(M_2)$ for penguin contractions.

The weak annihilation contributions to the decay $\bar{B} \to M_1 M_2$ ($M_1 M_2 = P_1 P_2,\ PV,\ VP$) can be described in terms of the building blocks b_j^p and $b_{j,\rm EW}^p$:

$$\frac{G_F}{\sqrt{2}} \sum_{p=u,c} \lambda_p^r \ \langle M_1 M_2 | \mathcal{T}_{\mathcal{B}}{}^p | \bar{B} \rangle \ = \ i \frac{G_F}{\sqrt{2}} \sum_{p=u,c} \lambda_p^r \ f_B f_{M_1} f_{M_2} \sum_j (d_j b_j^p + d_j' b_{j,\rm EW}^p). \tag{3}$$

The building blocks have the expressions [20]

$$\begin{aligned}
b_1 \ &= \ \frac{C_F}{N_c^2} c_1 A_1^i, \qquad\qquad b_3^p = \frac{C_F}{N_c^2} \left[c_3 A_1^i + c_5 (A_3^i + A_3^f) + N_c c_6 A_3^f \right], \\
b_2 \ &= \ \frac{C_F}{N_c^2} c_2 A_1^i, \qquad\qquad b_4^p = \frac{C_F}{N_c^2} \left[c_4 A_1^i + c_6 A_2^f \right], \\
b_{3,\rm EW}^p \ &= \ \frac{C_F}{N_c^2} \left[c_9 A_1^i + c_7 (A_3^i + A_3^f) + N_c c_8 A_3^i \right],
\end{aligned}$$

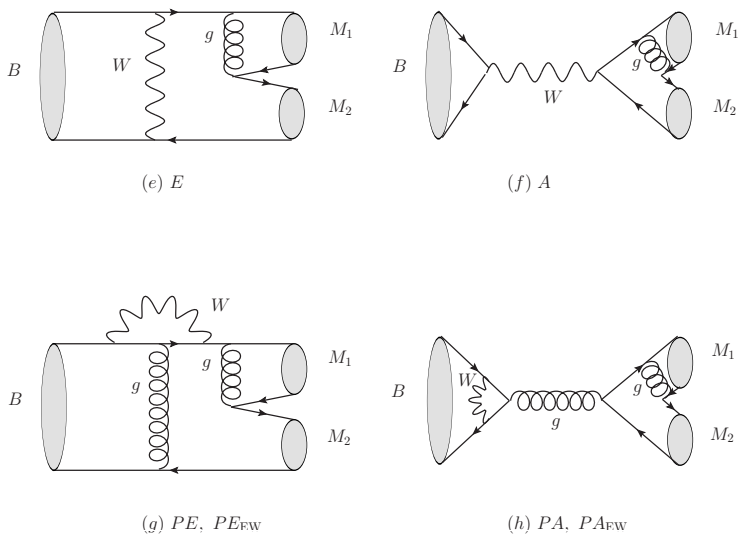

FIG. 2: (e) W-exchange [E], (f) W-annihilation [A], (g) QCD-penguin exchange [PE], (h) QCD-penguin annihilation [PA] diagrams. The EW-penguin exchange [$PE_{\rm EW}$] and EW-penguin annihilation [$PA_{\rm EW}$] diagrams are obtained from (g) and (h), respectively, by replacing the left gluon line by a single Z-boson or photon line. The gluon line of (e) and (f) and the right gluon line of (g) and (h) can be attached to the fermion lines in all possible ways.

$$b^p_{4,\rm EW} \;=\; \frac{C_F}{N_c^2}\left[c_{10}A^i_1 + c_8 A^i_2\right]. \tag{4}$$

The subscripts 1,2,3 of $A^{i,f}_n$ denote the annihilation amplitudes induced from $(V-A)(V-A)$, $(V-A)(V+A)$ and $(S-P)(S+P)$ operators, respectively, and the superscripts i and f refer to gluon emission from the initial and final-state quarks, respectively. We choose the convention that M_1 contains an antiquark from the weak vertex and M_2 contains a quark from the weak vertex, as in Ref. [21].

For the explicit expressions of vertex, hard spectator corrections and annihilation contributions, we refer to [20–22] for details. In practice, it is more convenient to express the decay amplitudes in terms of the flavor operators α^p_i and the annihilation operators β^p_j which are related to the coefficients a^p_i and b^p_j by

$$\begin{aligned}
\alpha_1(M_1M_2) \;&=\; a_1(M_1M_2)\;, \qquad\qquad \alpha_2(M_1M_2) = a_2(M_1M_2)\;,\\
\alpha^p_3(M_1M_2) \;&=\; \begin{cases} a^p_3(M_1M_2) - a^p_5(M_1M_2) & \text{for } M_1M_2 = PP,\ VP\;,\\ a^p_3(M_1M_2) + a^p_5(M_1M_2) & \text{for } M_1M_2 = PV\;, \end{cases}
\end{aligned}$$

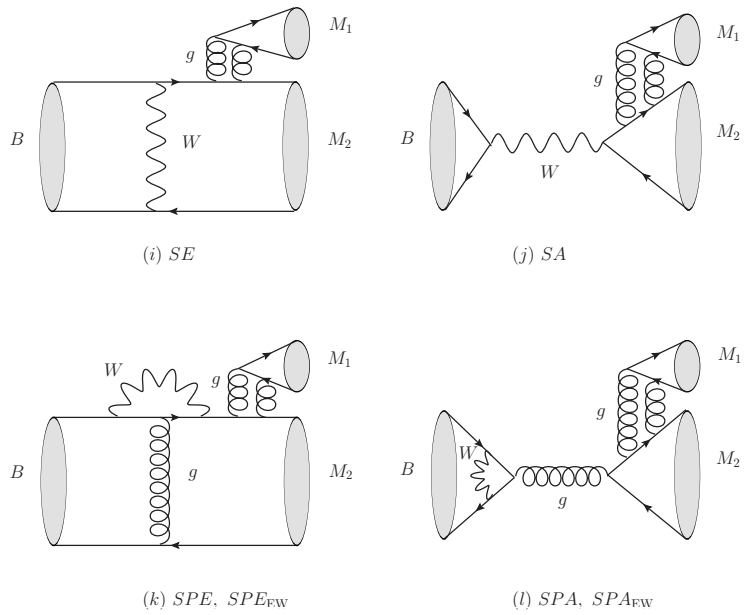

FIG. 3: (i) Flavor-singlet W-exchange [SE], (j) Flavor-singlet W-annihilation [SA], (k) Flavor-singlet QCD-penguin exchange [SPE], (l) Flavor-singlet QCD-penguin annihilation [SPA] diagrams. The Flavor-singlet EW-penguin exchange [$SPE_{\rm EW}$] and flavor-singlet EW-penguin annihilation [$SPA_{\rm EW}$] diagrams are obtained from (k) and (l), respectively, by replacing the leftest gluon line by a single Z-boson or photon line. The double gluon lines of (i), (j), (k) and (l) are shown for the case of $M_1 = P$. They are replaced by three gluon lines when $M_1 = V$. Each of the gluon lines of (i), (j), (k) and (l) can be separately attached to the fermion lines in all possible ways.

$$\alpha_4^p(M_1M_2) = \begin{cases} a_4^p(M_1M_2) + r_\chi^{M_2}\ a_6^p(M_1M_2) & \text{for } M_1M_2 = PP,\ PV\ , \\ a_4^p(M_1M_2) - r_\chi^{M_2}\ a_6^p(M_1M_2) & \text{for } M_1M_2 = VP\ , \end{cases}$$
$$\alpha_{3,\rm EW}^p(M_1M_2) = \begin{cases} a_9^p(M_1M_2) - a_7^p(M_1M_2) & \text{for } M_1M_2 = PP,\ VP\ , \\ a_9^p(M_1M_2) + a_7^p(M_1M_2) & \text{for } M_1M_2 = PV\ , \end{cases}$$
$$\alpha_{4,\rm EW}^p(M_1M_2) = \begin{cases} a_{10}^p(M_1M_2) + r_\chi^{M_2}\ a_8^p(M_1M_2) & \text{for } M_1M_2 = PP,\ PV\ , \\ a_{10}^p(M_1M_2) - r_\chi^{M_2}\ a_8^p(M_1M_2) & \text{for } M_1M_2 = VP\ , \end{cases} \tag{5}$$

and

$$\beta_j^p(M_1M_2) = \frac{if_Bf_{M_1}f_{M_2}}{X^{(\bar BM_1,M_2)}}\ b_j^p(M_1M_2)\ , \tag{6}$$

where f_M is the decay constant of a meson M and the chiral factors $r_\chi^{M_2}$ are given by

$$r_\chi^P(\mu) = \frac{2m_P^2}{m_b(\mu)(m_2+m_1)(\mu)}, \qquad r_\chi^V(\mu) = \frac{2m_V}{m_b(\mu)}\ \frac{f_V^\perp(\mu)}{f_V}\ , \tag{7}$$

with $f_V^\perp(\mu)$ being the scale-dependent transverse decay constant of the vector meson V. The relevant factorizable matrix elements are

$$\begin{aligned} X^{(\bar{B}P_1,P_2)} &\equiv \langle P_2|J^\mu|0\rangle\langle P_1|J'_\mu|\overline{B}\rangle = if_{P_2}(m_B^2 - m_{P_1}^2)\ F_0^{BP_1}(m_{P_2}^2)\ , \\ X^{(\bar{B}P,V)} &\equiv \langle V|J^\mu|0\rangle\langle P|J'_\mu|\overline{B}\rangle = 2f_V\ m_B p_c\ F_1^{BP}(m_V^2)\ , \\ X^{(\bar{B}V,P)} &\equiv \langle P|J^\mu|0\rangle\langle V|J'_\mu|\overline{B}\rangle = 2f_P\ m_B p_c\ A_0^{BV}(m_P^2)\ , \end{aligned} \tag{8}$$

with p_c being the c.m. momentum. Here we have followed the conventional Bauer-Stech-Wirbel definition for form factors $F_{0,1}^{BP}$ and A_0^{BV} [23].

A. SU(3)$_{\rm F}$ decomposition of decay amplitudes

The decay amplitudes of $\bar{B}_{u,d}(\bar{B}_s) \to M_1M_2$ modes can be analyzed by the relevant quark diagrams and written in terms of the SU(3)$_{\rm F}$ amplitudes. The decomposition of the decay amplitudes of these modes is displayed in Tables I−XXIV. In these tables, the subscript M_1 (or M_2) of the amplitudes $T^{(\zeta)}_{M_1\ [M_2]}$, $\cdots$, etc., represents the case that the meson M_1 (or M_2) contains the spectator quark in the final state. The superscript ζ of the amplitudes is only applied to the case involving an $\eta^{(\prime)}$ or an ω/ϕ, or both $\eta^{(\prime)}$ and ω/ϕ in the final state and denotes the quark content ($\zeta = q, s, c$) of $\eta^{(\prime)}$ and ω/ϕ with $q = u$ or d. The value of ζ is shown in the parenthesis as (q), (s) or (c). For $\bar{B}^0(\bar{B}_s) \to \eta^{(\prime)}\eta^{(\prime)}$, two values of ζ are shown in one parenthesis: e.g., (q, s), where q and s denote the quark content of the first and second $\eta^{(\prime)}$, respectively. A similar rule is also applied to the case of $\bar{B}^0(\bar{B}_s) \to \eta^{(\prime)}\ \omega/\phi$. On the other hand, to distinguish the decays with $|\Delta S| = 1$ from those with $\Delta S = 0$, we will put the prime to all the SU(3)$_{\rm F}$ amplitudes for the former, for example $T'^{(\zeta)}_{M_1\ [M_2]}$. The SU(3)$_{\rm F}$-singlet amplitudes $S^{(\prime)}_{M_1[M_2]}$ are involved only when the SU(3)$_{\rm F}$-singlet meson(s) ($\eta,\ \eta',\ \omega,\ \phi$) appear(s) in the final state.

We will give some examples for illustration. The decay amplitude of $B^- \to \pi^-\bar{K}^0$ which is a $\bar{B}_u \to PP$ mode with $|\Delta S| = 1$ can be written, from Tables IV−V, as

$$\mathcal{A}_{B^-\to\pi^-\bar{K}^0} \ = \ P'_\pi - \frac{1}{3}P^{C\prime}_{{\rm EW},\pi} + A'_\pi + PE'_\pi + \frac{2}{3}PE'_{{\rm EW},\pi}\ . \tag{9}$$

The decay amplitude of $\bar{B}^0 \to \eta^{(\prime)}\bar{K}^{*0}$ which is a $\bar{B}_d \to PV$ mode with $|\Delta S| = 1$ can be recast, from Tables X−XII, to

$$\sqrt{2}\ \mathcal{A}_{\bar{B}^0\to\eta^{(\prime)}\bar{K}^{*0}}$$

$$
\begin{aligned}
&= \left(C'^{(q)}_{K^*} + 2S'^{(q)}_{K^*} + \frac{1}{3}P'^{(q)}_{\rm EW,\ K^*} + 2SPE'^{(q)}_{K^*} - \frac{2}{3}SPE'^{(q)}_{\rm EW,\ K^*}\right) \\
&\quad +\sqrt{2}\left(S'^{(s)}_{K^*} + P'^{(s)}_{K^*} - \frac{1}{3}P'^{(s)}_{\rm EW,\ K^*} - \frac{1}{3}P^{C\prime,\ (s)}_{\rm EW,\ K^*} + PE'^{(s)}_{K^*} - \frac{1}{3}PE'^{(s)}_{\rm EW,\ K^*}\right. \\
&\quad \left. +SPE'^{(s)}_{K^*} - \frac{1}{3}SPE'^{(s)}_{\rm EW,\ K^*}\right) \\
&\quad +\sqrt{2}\left(C'^{(c)}_{K^*} + S'^{(c)}_{K^*}\right) \\
&\quad +\left(P'^{(q)}_{\eta^{(\prime)}} - \frac{1}{3}P^{C\prime,\ (q)}_{\rm EW,\ \eta^{(\prime)}} + PE'^{(q)}_{\eta^{(\prime)}} - \frac{1}{3}PE'^{(q)}_{\rm EW,\ \eta^{(\prime)}}\right) ,
\end{aligned} \tag{10}
$$

where the superscripts (q), (s) and (c) represent the quark contents of $\eta^{(\prime)}$, such as $\eta_q^{(\prime)}$, $\eta_s^{(\prime)}$ and $\eta_c^{(\prime)}$, respectively. Likewise, from Tables VII−IX, the decay amplitude of $\bar{B}^0 \to \eta^{(\prime)}\ \omega/\phi$ which is a $\bar{B}_d \to PV$ mode with $\Delta S = 0$ is given by

$$
\begin{aligned}
2\ \mathcal{A}_{\bar{B}^0\to\eta^{(\prime)}\ \omega/\phi} &= \left(C^{(q,\ q)}_{\eta^{(\prime)}} + 2S^{(q,\ q)}_{\eta^{(\prime)}} + P^{(q,\ q)}_{\eta^{(\prime)}} + \frac{1}{3}P^{(q,\ q)}_{\rm EW,\ \eta^{(\prime)}} - \frac{1}{3}P^{C,\ (q,\ q)}_{\rm EW,\ \eta^{(\prime)}}\right. \\
&\quad +E^{(q,\ q)}_{\eta^{(\prime)}} + PE^{(q,\ q)}_{\eta^{(\prime)}} + 2PA^{(q,\ q)}_{\eta^{(\prime)}} - \frac{1}{3}PE^{(q,\ q)}_{\rm EW,\ \eta^{(\prime)}} + \frac{1}{3}PA^{(q,\ q)}_{\rm EW,\ \eta^{(\prime)}} \\
&\quad \left. +2SE^{(q,\ q)}_{\eta^{(\prime)}} + 2SPE^{(q,\ q)}_{\eta^{(\prime)}} + 4SPA^{(q,\ q)}_{\eta^{(\prime)}} - \frac{2}{3}SPE^{(q,\ q)}_{\rm EW,\ \eta^{(\prime)}} + \frac{2}{3}SPA^{(q,\ q)}_{\rm EW,\ \eta^{(\prime)}}\right) \\
&+ \sqrt{2}\left(S^{(q,\ s)}_{\eta^{(\prime)}} - \frac{1}{3}P^{(q,\ s)}_{\rm EW,\ \eta^{(\prime)}} + SE^{(q,\ s)}_{\eta^{(\prime)}} + SPE^{(q,\ s)}_{\eta^{(\prime)}} + 2SPA^{(q,\ s)}_{\eta^{(\prime)}}\right. \\
&\quad \left. -\frac{1}{3}SPE^{(q,\ s)}_{\rm EW,\ \eta^{(\prime)}} + \frac{1}{3}SPA^{(q,\ s)}_{\rm EW,\ \eta^{(\prime)}}\right) \\
&+ \sqrt{2}\left(2SPA^{(s,\ q)}_{\eta^{(\prime)}} - \frac{2}{3}SPA^{(s,\ q)}_{\rm EW,\ \eta^{(\prime)}}\right) \\
&+ 2\left(PA^{(s,\ s)}_{\eta^{(\prime)}} - \frac{1}{3}PA^{(s,\ s)}_{\rm EW,\ \eta^{(\prime)}} + SPA^{(s,\ s)}_{\eta^{(\prime)}} - \frac{1}{3}SPA^{(s,\ s)}_{\rm EW,\ \eta^{(\prime)}}\right) \\
&+ \left(C^{(q,\ q)}_{\omega/\phi} + 2S^{(q,\ q)}_{\omega/\phi} + P^{(q,\ q)}_{\omega/\phi} + \frac{1}{3}P^{(q,\ q)}_{\rm EW,\ \omega/\phi} - \frac{1}{3}P^{C,\ (q,\ q)}_{\rm EW,\ \omega/\phi}\right. \\
&\quad +E^{(q,\ q)}_{\omega/\phi} + PE^{(q,\ q)}_{\omega/\phi} + 2PA^{(q,\ q)}_{\omega/\phi} - \frac{1}{3}PE^{(q,\ q)}_{\rm EW,\ \omega/\phi} + \frac{1}{3}PA^{(q,\ q)}_{\rm EW,\ \omega/\phi} \\
&\quad \left. +2SE^{(q,\ q)}_{\omega/\phi} + 2SPE^{(q,\ q)}_{\omega/\phi} + 4SPA^{(q,\ q)}_{\omega/\phi} - \frac{2}{3}SPE^{(q,\ q)}_{\rm EW,\ \omega/\phi} + \frac{2}{3}SPA^{(q,\ q)}_{\rm EW,\ \omega/\phi}\right) \\
&+ \sqrt{2}\left(S^{(q,\ s)}_{\omega/\phi} - \frac{1}{3}P^{(q,\ s)}_{\rm EW,\ \omega/\phi} + SE^{(q,\ s)}_{\omega/\phi} + SPE^{(q,\ s)}_{\omega/\phi} + 2SPA^{(q,\ s)}_{\omega/\phi}\right. \\
&\quad \left. -\frac{1}{3}SPE^{(q,\ s)}_{\rm EW,\ \omega/\phi} + \frac{1}{3}SPA^{(q,\ s)}_{\rm EW,\ \omega/\phi}\right) \\
&+ \sqrt{2}\left(C^{(q,\ c)}_{\omega/\phi} + S^{(q,\ c)}_{\omega/\phi}\right) \\
&+ \sqrt{2}\left(2SPA^{(s,\ q)}_{\omega/\phi} - \frac{2}{3}SPA^{(s,\ q)}_{\rm EW,\ \omega/\phi}\right) \\
&+ 2\left(PA^{(s,\ s)}_{\omega/\phi} - \frac{1}{3}PA^{(s,\ s)}_{\rm EW,\ \omega/\phi} + SPA^{(s,\ s)}_{\omega/\phi} - \frac{1}{3}SPA^{(s,\ s)}_{\rm EW,\ \omega/\phi}\right) ,
\end{aligned} \tag{11}
$$

where the superscripts $(q',\ q'')$ with $q', q'' = q, s$ denote the quark contents of $(\eta^{(\prime)},\ \omega/\phi)$, such as $(\eta_q^{(\prime)},\ \omega_q/\phi_q)$, $(\eta_q^{(\prime)},\ \omega_s/\phi_s)$, etc. When ideal mixing for ω and ϕ is assumed, ω_s and

ϕ_q terms vanish: i.e., the amplitudes with the superscripts $(q,\ s)$ or $(s,\ s)$ for $B \to \eta^{(\prime)}\omega$ and the superscripts $(q,\ q)$ or $(s,\ q)$ for $B \to \eta^{(\prime)}\phi$ are set to be zero.

B. The SU(3)$_{\rm F}$ amplitudes and QCD factorization

The SU(3)$_{\rm F}$ amplitudes for $\bar{B}_{u,d}(\bar{B}_s) \to M_1 M_2$ (with $M_1M_2 = P_1P_2,\ PV,\ VP$) decays can be expressed in terms of the quantities calculated in the framework of QCD factorization as follows: [4]

$$
\begin{aligned}
T^{(\zeta)}_{M_1[M_2]} &= \frac{G_F}{\sqrt{2}}\ \lambda_u^r\ \alpha_1(M_1M_2)\ X^{(\bar{B}M_1,\ M_2)}\ [X^{(\bar{B}M_2,\ M_1)}]\ , \\
C^{(\zeta)}_{M_1[M_2]} &= \frac{G_F}{\sqrt{2}}\ \lambda_u^r\ \alpha_2(M_1M_2)\ X^{(\bar{B}M_1,\ M_2)}\ [X^{(\bar{B}M_2,\ M_1)}]\ , \\
S^{(\zeta)}_{M_1[M_2]} &= \frac{G_F}{\sqrt{2}}\ \sum_{p=u,c}\ \lambda_p^r\ \alpha_3^p(M_1M_2)\ X^{(\bar{B}M_1,\ M_2)}\ [X^{(\bar{B}M_2,\ M_1)}]\ , \\
P^{(\zeta)}_{M_1[M_2]} &= \frac{G_F}{\sqrt{2}}\ \sum_{p=u,c}\ \lambda_p^r\ \alpha_4^p(M_1M_2)\ X^{(\bar{B}M_1,\ M_2)}\ [X^{(\bar{B}M_2,\ M_1)}]\ , \\
P^{(\zeta)}_{{\rm EW},M_1[M_2]} &= \frac{G_F}{\sqrt{2}}\ \sum_{p=u,c}\ \lambda_p^r\ \frac{3}{2}\alpha_{3,{\rm EW}}^p(M_1M_2)\ X^{(\bar{B}M_1,\ M_2)}\ [X^{(\bar{B}M_2,\ M_1)}]\ , \\
P^{C,\ (\zeta)}_{{\rm EW},M_1[M_2]} &= \frac{G_F}{\sqrt{2}}\ \sum_{p=u,c}\ \lambda_p^r\ \frac{3}{2}\alpha_{4,{\rm EW}}^p(M_1M_2)\ X^{(\bar{B}M_1,\ M_2)}\ [X^{(\bar{B}M_2,\ M_1)}]\ ,
\end{aligned}
\tag{12}
$$

where the superscript $\zeta = q, s, c$, which is only applied to the case when M_1 (or M_2) $= \eta^{(\prime)}$ or ω/ϕ, or $M_1M_2 = \eta^{(\prime)}\eta^{(\prime)}$ or $\eta^{(\prime)}\omega/\phi$. As mentioned before, for $|\Delta S| = 1$ decays, we will put the prime to all the SU(3)$_{\rm F}$ amplitudes. The *unprimed* and *primed* amplitudes have the CKM factor $\lambda_p^r \equiv V_{pb}V_{pr}^*$ with $r = d$ and $r = s$, respectively. The weak annihilation amplitudes are given by

$$
\begin{aligned}
E^{(\zeta)}_{M_1[M_2]} &= \frac{G_F}{\sqrt{2}}\ \lambda_u^r\ (if_Bf_{M_1}f_{M_2})\ [b_1]_{M_1M_2\ [M_2M_1]}\ , \\
A^{(\zeta)}_{M_1[M_2]} &= \frac{G_F}{\sqrt{2}}\ \lambda_u^r\ (if_Bf_{M_1}f_{M_2})\ [b_2]_{M_1M_2\ [M_2M_1]}\ , \\
PE^{(\zeta)}_{M_1[M_2]} &= \frac{G_F}{\sqrt{2}}\ \sum_{p=u,c}\lambda_p^r\ (if_Bf_{M_1}f_{M_2})\ [b_3^p]_{M_1M_2\ [M_2M_1]}\ , \\
PA^{(\zeta)}_{M_1[M_2]} &= \frac{G_F}{\sqrt{2}}\ \sum_{p=u,c}\lambda_p^r\ (if_Bf_{M_1}f_{M_2})\ [b_4^p]_{M_1M_2\ [M_2M_1]}\ , \\
PE^{(\zeta)}_{{\rm EW},M_1[M_2]} &= \frac{G_F}{\sqrt{2}}\ \sum_{p=u,c}\lambda_p^r\ (if_Bf_{M_1}f_{M_2})\ \left[\frac{3}{2}b_{3,{\rm EW}}^p\right]_{M_1M_2\ [M_2M_1]}\ ,
\end{aligned}
$$

[4] The factorizable amplitude $X^{(\bar{B}M_1,\ M_2)}$ is denoted by $A_{M_1M_2}$ in [21].

$$PA^{(\zeta)}_{\rm EW,M_1[M_2]} = \frac{G_F}{\sqrt{2}} \sum_{p=u,c} \lambda_p^r \ (if_B f_{M_1} f_{M_2}) \ \left[\frac{3}{2} b^p_{4,\rm EW}\right]_{M_1M_2 \ [M_2M_1]} \ , \tag{13}$$

and the singlet weak annihilation amplitudes by

$$\begin{aligned}
SE^{(\zeta)}_{M_1[M_2]} &= \frac{G_F}{\sqrt{2}} \ \lambda_u^r \ (if_B f_{M_1} f_{M_2}) \ [b_{S1}]_{M_1M_2 \ [M_2M_1]} \ , \\
SA^{(\zeta)}_{M_1[M_2]} &= \frac{G_F}{\sqrt{2}} \ \lambda_u^r \ (if_B f_{M_1} f_{M_2}) \ [b_{S2}]_{M_1M_2 \ [M_2M_1]} \ , \\
SPE^{(\zeta)}_{M_1[M_2]} &= \frac{G_F}{\sqrt{2}} \sum_{p=u,c} \lambda_p^r \ (if_B f_{M_1} f_{M_2}) \ [b^p_{S3}]_{M_1M_2 \ [M_2M_1]} \ , \\
SPA^{(\zeta)}_{M_1[M_2]} &= \frac{G_F}{\sqrt{2}} \sum_{p=u,c} \lambda_p^r \ (if_B f_{M_1} f_{M_2}) \ [b^p_{S4}]_{M_1M_2 \ [M_2M_1]} \ , \\
SPE^{(\zeta)}_{\rm EW,M_1[M_2]} &= \frac{G_F}{\sqrt{2}} \sum_{p=u,c} \lambda_p^r \ (if_B f_{M_1} f_{M_2}) \ \left[\frac{3}{2} b^p_{S3,\rm EW}\right]_{M_1M_2 \ [M_2M_1]} \ , \\
SPA^{(\zeta)}_{\rm EW,M_1[M_2]} &= \frac{G_F}{\sqrt{2}} \sum_{p=u,c} \lambda_p^r \ (if_B f_{M_1} f_{M_2}) \ \left[\frac{3}{2} b^p_{S4,\rm EW}\right]_{M_1M_2 \ [M_2M_1]} \ ,
\end{aligned} \tag{14}$$

where we have used the notation $[b^p_j]_{M_1M_2} \equiv b^p_j(M_1, M_2)$. Note that the weak annihilation contributions in the QCDF approach given in Eq. (3) include all the above $\mathrm{SU(3)_F}$ amplitudes given in Eqs. (13) and (14), such as $E^{(\prime)}_{M_i}$, $A^{(\prime)}_{M_i}$, ..., $SE^{(\prime)}_{M_i}$, $SA^{(\prime)}_{M_i}$, $\cdots$, etc.

Using the above relations, one can easily translate the decay amplitude expressed in terms of the $\mathrm{SU(3)_F}$ amplitudes as shown in Tables I−XXIV into that expressed in terms of the quantities calculated in the framework of QCDF. For example, the decay amplitude of $B^- \to \pi^- \bar{K}^0$ given in Eq. (9) can be rewritten in terms of the quantities calculated in QCDF:

$$\mathcal{A}_{B^-\to\pi^-\bar{K}^0} = \frac{G_F}{\sqrt{2}} \sum_{p=u,c} \lambda_p^s \Big[\delta_{pu} \ \beta_2 + \alpha_4^p - \frac{1}{2}\alpha^p_{4,\rm EW} + \beta_3^p + \beta^p_{3,\rm EW}\Big] \ X^{(\bar{B}\pi, \ \bar{K})} \ . \tag{15}$$

Likewise, the decay amplitude of $\bar{B}^0 \to \eta^{(\prime)} \bar{K}^{*0}$ in Eq. (10) now reads

$$\begin{aligned}
&\sqrt{2} \ \mathcal{A}_{\bar{B}^0\to\eta^{(\prime)}\bar{K}^{*0}} \\
&= \frac{G_F}{\sqrt{2}} \sum_{p=u,c} \lambda_p^s \Bigg\{ \Big[\delta_{pu} \ \alpha_2 + 2\alpha_3^p + \frac{1}{2}\alpha^p_{3,\rm EW} + \beta_3^p + \beta^p_{3,\rm EW}\Big] \ X^{(\bar{B}K^*, \ \eta_q^{(\prime)})} \\
&\quad + \sqrt{2} \ \Big[\alpha_3^p + \alpha_4^p - \frac{1}{2}\alpha^p_{3,\rm EW} - \frac{1}{2}\alpha^p_{4,\rm EW} + \beta_3^p - \frac{1}{2}\beta^p_{3,\rm EW} + \beta^p_{S3} - \frac{1}{2}\beta^p_{S3,\rm EW}\Big] \ X^{(\bar{B}K^*, \ \eta_s^{(\prime)})} \\
&\quad + \sqrt{2} \ \Big[\delta_{pc} \ \alpha_2 + \alpha_3^p\Big] \ X^{(\bar{B}K^*, \ \eta_c^{(\prime)})} \\
&\quad + \Big[\alpha_4^p - \frac{1}{2}\alpha^p_{4,\rm EW} + \beta_3^p - \frac{1}{2}\beta^p_{3,\rm EW}\Big] \ X^{(\bar{B}\eta_q^{(\prime)}, \ K^*)} \Bigg\} \ .
\end{aligned} \tag{16}$$

Finally, the decay amplitude of $\bar{B}^0 \to \eta^{(\prime)}\ \omega/\phi$ in Eq. (11) is recast to

$$
\begin{aligned}
&2\ \mathcal{A}_{\bar{B}^0\to\eta^{(\prime)}\ \omega/\phi} \\
&= \frac{G_F}{\sqrt{2}} \sum_{p=u,c} \lambda_p^d \Bigg\{ \Big[\delta_{pu}\ (\alpha_2+\beta_1+2\beta_{S1}) + 2\alpha_3^p + \alpha_4^p + \frac{1}{2}\alpha_{3,\rm EW}^p - \frac{1}{2}\alpha_{4,\rm EW}^p \\
&\qquad +\beta_3^p + 2\beta_4^p - \frac{1}{2}\beta_{3,\rm EW}^p + \frac{1}{2}\beta_{4,\rm EW}^p + 2\beta_{S3}^p + 4\beta_{S4}^p - \beta_{S3,\rm EW}^p + \beta_{S4,\rm EW}^p \Big]\ X^{(\bar{B}\eta_q^{(\prime)},\ \omega_q/\phi_q)} \\
&+\sqrt{2}\ \Big[\delta_{pu}\ \beta_{S1} + \alpha_3^p - \frac{1}{2}\alpha_{3,\rm EW}^p + \beta_{S3} + 2\beta_{S4}^p - \frac{1}{2}\beta_{S3,\rm EW}^p + \frac{1}{2}\beta_{S4,\rm EW}^p \Big]\ X^{(\bar{B}\eta_q^{(\prime)},\ \omega_s/\phi_s)} \\
&+\sqrt{2}\ (-if_B f_{\eta^{(\prime)}} f_{\omega/\phi}) \left[2b_{S4}^p - b_{S4,\rm EW}^p \right]_{\eta_s^{(\prime)}\ \omega_q/\phi_q} \\
&+2\ (-if_B f_{\eta^{(\prime)}} f_{\omega/\phi}) \left[b_4^p - \frac{1}{2}b_{4,\rm EW}^p + b_{S4}^p - \frac{1}{2}b_{S4,\rm EW}^p \right]_{\eta_s^{(\prime)}\ \omega_s/\phi_s} \\
&+\Big[\delta_{pu}\ (\alpha_2+\beta_1+2\beta_{S1}) + 2\alpha_3^p + \alpha_4^p + \frac{1}{2}\alpha_{3,\rm EW}^p - \frac{1}{2}\alpha_{4,\rm EW}^p \\
&\qquad +\beta_3^p + 2\beta_4^p - \frac{1}{2}\beta_{3,\rm EW}^p + \frac{1}{2}\beta_{4,\rm EW}^p + 2\beta_{S3}^p + 4\beta_{S4}^p - \beta_{S3,\rm EW}^p + \beta_{S4,\rm EW}^p \Big]\ X^{(\bar{B}\ \omega_q/\phi_q,\ \eta_q^{(\prime)})} \\
&+\sqrt{2}\ \Big[\delta_{pu}\ \beta_{S1} + \alpha_3^p - \frac{1}{2}\alpha_{3,\rm EW}^p + \beta_{S3} + 2\beta_{S4}^p - \frac{1}{2}\beta_{S3,\rm EW}^p + \frac{1}{2}\beta_{S4,\rm EW}^p \Big]\ X^{(\bar{B}\ \omega_q/\phi_q,\ \eta_s^{(\prime)})} \\
&+\sqrt{2}\ \Big[\delta_{pc}\ \alpha_2 + \alpha_3^p \Big]\ X^{(\bar{B}\ \omega_q/\phi_q,\ \eta_c^{(\prime)})} \\
&+\sqrt{2}\ (-if_B f_{\eta^{(\prime)}} f_{\omega/\phi}) \left[2b_{S4}^p - b_{S4,\rm EW}^p \right]_{\omega_s/\phi_s,\ \eta_q^{(\prime)}} \\
&+2\ (-if_B f_{\eta^{(\prime)}} f_{\omega/\phi}) \left[b_4^p - \frac{1}{2}b_{4,\rm EW}^p + b_{S4}^p - \frac{1}{2}b_{S4,\rm EW}^p \right]_{\omega_s/\phi_s,\ \eta_s^{(\prime)}} \Bigg\} . \qquad (17)
\end{aligned}
$$

All the decay amplitudes of $\bar{B} \to PP, VP$ in QCD factorization shown in Appendix A of Ref. [21] can be obtained from the $SU(3)_{\rm F}$ amplitudes displayed in Tables I−XXIV.

III. NUMERICAL ANALYSIS OF FLAVOR SU(3) AMPLITUDES IN QCDF

In this section we estimate the magnitude of each $\rm SU(3)_F$ amplitude in the framework of QCDF by using the relations given in Eqs. (12), (13) and (14). For the numerical analysis, we shall use the same input values for the relevant parameters as those in Ref. [24]. Specifically we use the values of the form factors for $B_{u,d} \to P$ and $B_{u,d} \to V$ transitions obtained in the light-cone QCD sum rules [25] and those for $B_s \to V$ transitions obtained in the covariant light-front quark model [26] with some modifications :

$$
F_0^{B\pi}(0) = 0.25\ , \qquad F_0^{BK}(0) = 0.35\ , \qquad F_0^{B\eta_q}(0) = 0.296\ ,
$$

$$
\begin{aligned}
&F_0^{B_sK}(0) = 0.24 \ , \qquad F_0^{B_s\eta_s}(0) = 0.28 \ , \\
&A_0^{B\rho}(0) = 0.303 \ , \qquad A_0^{BK^*}(0) = 0.374 \ , \qquad A_0^{B\omega}(0) = 0.281 \ , \\
&A_0^{B_sK^*}(0) = 0.30 \ , \qquad A_0^{B_s\phi}(0) = 0.32 \ .
\end{aligned} \tag{18}
$$

Here for $\eta^{(\prime)}$ we have used the flavor states $q\bar{q} \equiv (u\bar{u} + d\bar{d})/\sqrt{2}$, $s\bar{s}$ and $c\bar{c}$ labeled by the η_q, η_s and η_c, respectively, and the form factors for $B \to \eta^{(\prime)}$ are given by

$$
\begin{aligned}
&F^{B\eta} = F^{B\eta_q} \cos\theta \ , \qquad F^{B\eta'} = F^{B\eta_q} \sin\theta \ , \\
&F^{B_s\eta} = -F^{B_s\eta_s} \sin\theta \ , \qquad F^{B_s\eta'} = F^{B_s\eta_s} \cos\theta \ ,
\end{aligned} \tag{19}
$$

where the small mixing with η_c is neglected and the η_q-η_s mixing angle θ defined by

$$
\begin{aligned}
|\eta\rangle &= \cos\theta|\eta_q\rangle - \sin\theta|\eta_s\rangle, \\
|\eta'\rangle &= \sin\theta|\eta_q\rangle + \cos\theta|\eta_s\rangle,
\end{aligned} \tag{20}
$$

is $(39.3 \pm 1.0)^\circ$ in the Feldmann-Kroll-Stech mixing scheme [27]. For the decay constants, we use the values (in units of MeV) [27, 28]

$$
\begin{aligned}
&f_\pi = 132 \ , \qquad f_K = 160 \ , \qquad f_{B_{u,d}} = 210 \ , \qquad f_{B_s} = 230 \ , \\
&f_{\eta'}^q = 107 \ , \qquad f_\eta^q = 89 \ , \qquad f_{\eta'}^s = -112 \ , \qquad f_\eta^s = 137 \ , \\
&f_\rho = 216 \ , \qquad f_{K^*} = 220 \ , \qquad f_\omega = 187 \ , \qquad f_\phi = 215 \ .
\end{aligned} \tag{21}
$$

It is known that although physics behind nonleptonic B decays is extremely complicated, it is greatly simplified in the heavy quark limit $m_b \to \infty$ as the decay amplitude becomes factorizable and can be expressed in terms of decay constants and form factors. However, this simple approach encounters three major difficulties: (i) the predicted branching fractions for penguin-dominated $\bar{B} \to PP$, VP, VV decays are systematically below the measurements [21] (ii) direct CP-violating asymmetries for $\bar{B}^0 \to K^-\pi^+$, $\bar{B}^0 \to K^{*-}\pi^+$, $B^- \to K^-\rho^0$, $\bar{B}^0 \to \pi^+\pi^-$ and $\bar{B}_s^0 \to K^+\pi^-$ disagree with experiment in signs [29], and (iii) the transverse polarization fraction in penguin-dominated charmless $\bar{B} \to VV$ decays is predicted to be very small, while experimentally it is comparable to the longitudinal polarization one. All these indicate the necessity of going beyond zeroth $1/m_b$ power expansion. In the QCDF approach one considers the power correction to penguin amplitudes due to weak penguin annihilation characterized by the parameter β_3^p or b_3^p. However, QCD-penguin exchange

amplitudes involve troublesome endpoint divergences and hence they can be studied only in a phenomenological way. We shall follow [20] to model the endpoint divergence $X \equiv \int_0^1 dx/\bar{x}$ in the annihilation diagrams as

$$X_A = \ln\left(\frac{m_B}{\Lambda_h}\right)(1+\rho_A e^{i\phi_A}), \tag{22}$$

where Λ_h is a typical scale of order 500 MeV, and ρ_A and ϕ_A are the unknown real parameters.

By adjusting the magnitude ρ_A and the phase ϕ_A in this scenario, all the above-mentioned difficulties can be resolved. However, a scrutiny of the QCDF predictions reveals more puzzles with respect to direct CP violation, as pointed out in [24, 29]. While the signs of CP asymmetries in $K^-\pi^+,\ K^-\rho^0$ modes are flipped to the right ones in the presence of power corrections from penguin annihilation, the signs of A_{CP} in $B^- \to K^-\pi^0,\ K^-\eta,\ \pi^-\eta$ and $\bar{B}^0 \to \pi^0\pi^0,\ \bar{K}^{*0}\eta$ will also get reversed in such a way that they disagree with experiment. This indicates that it is necessary to consider subleading power corrections other than penguin annihilation. It turns out that an additional subleading $1/m_b$ power correction to color-suppressed tree amplitudes is crucial for resolving the aforementioned CP puzzles and explaining the decay rates for the color-suppressed tree-dominated $\pi^0\pi^0$, $\rho^0\pi^0$ modes [24, 29]. A solution to the $B \to K\pi$ CP-puzzle related to the difference of CP asymmetries of $B^- \to K^-\pi^0$ and $\bar{B}^0 \to K^-\pi^+$ requires a large complex color-suppressed tree amplitude and/or a large complex electroweak penguin. These two possibilities can be discriminated in tree-dominated B decays. The CP puzzles with $\pi^-\eta$, $\pi^0\pi^0$ and the rate deficit problems with $\pi^0\pi^0,\ \rho^0\pi^0$ can only be resolved by having a large complex color-suppressed tree topology C. While the New Physics solution to the $B \to K\pi$ CP puzzle is interesting, it is most likely irrelevant for tree-dominated decays.

We shall use the fitted values of the parameters ρ_A and ϕ_A given in [24]:

$$\begin{aligned}
&\text{For } \bar{B}_{u,d}(\bar{B}_s) \to PP\ , \qquad \rho_A = 1.10\ (1.00)\ , \quad \phi_A = -50^\circ\ (-55^\circ)\ ,\\
&\text{For } \bar{B}_{u,d}(\bar{B}_s) \to VP\ , \qquad \rho_A = 1.07\ (0.90)\ , \quad \phi_A = -70^\circ\ (-65^\circ)\ ,\\
&\text{For } \bar{B}_{u,d}(\bar{B}_s) \to PV\ , \qquad \rho_A = 0.87\ (0.85)\ , \quad \phi_A = -30^\circ\ (-30^\circ)\ .
\end{aligned} \tag{23}$$

Following [29], power corrections to the color-suppressed topology are parametrized as

$$a_2 \to a_2(1+\rho_C e^{i\phi_C}), \tag{24}$$

with the unknown parameters ρ_C and ϕ_C to be inferred from experiment. We shall use [29]

$$\rho_C \approx 1.3\,,\ 0.8\,,\ 0, \qquad \phi_C \approx -70^\circ\,, -80^\circ\,,\ 0, \tag{25}$$

for $\bar{B} \to PP,\ VP,\ VV$ decays, respectively.

A. Magnitudes and strong phases of the SU(3)$_{\rm F}$ amplitudes

From Eqs. (12)−(14), it is obvious that the SU(3)$_{\rm F}$ amplitudes for $\bar{B}_{u,d}(B_s) \to M_1 M_2$ depend on the specific final states M_1 and M_2. Thus, the magnitudes of these SU(3)$_F$ amplitudes are process-dependent in general, though numerically the dependence turns out to be moderate. In order to find typical magnitudes of these SU(3)$_{\rm F}$ ones, we choose typical decay processes as explained below, and use only the central values of the input parameters. ¿From now on, we shall use a notation for the relevant strong and weak phases as follows: e.g., the color-favored tree amplitude for $\Delta S = 0$ ($|\Delta S| = 1$) decays is denoted as $T_P^{(\prime)} \equiv |T_P^{(\prime)}|\ e^{i\left(\delta_P^{T^{(\prime)}} + \theta^{T^{(\prime)}}\right)}$ with the strong phase $\delta_P^{T^{(\prime)}}$ and the weak phase $\theta^{T^{(\prime)}} = \arg(V_{ub}V_{ud(s)}^*)$.

The numerical estimates of the SU(3)$_{\rm F}$ amplitudes are displayed in Tables XXV−XXVIII. In the case of $\bar{B}_{u,d}(\bar{B}_s) \to P_1 P_2$ decays with $\Delta S = 0$, the modes $\bar{B}_{u,d}(\bar{B}_s) \to \pi\pi\ (\pi K)$ are used to numerically compute the relevant SU(3)$_{\rm F}$ amplitudes such as T_P, C_P, P_P and so on, except for $S_P^{(q,s,c)}$ which $\bar{B}_{u,d}(\bar{B}_s) \to \pi\eta\ (K\eta)$ are used for. Similarly, for $|\Delta S| = 1$ decays the processes $\bar{B}_{u,d}(\bar{B}_s) \to \pi K\ (KK)$ are used to estimate T'_P, C'_P, P'_P and so on, except for $S_P^{\prime(q,s,c)}$ which $\bar{B}_{u,d}(\bar{B}_s) \to K\eta\ (\eta\eta)$ are used for. In the case of $\Delta S = 0$ $\bar{B}_{u,d}(\bar{B}_s) \to PV$ decays, the modes $\bar{B}_{u,d}(\bar{B}_s) \to \pi\rho\ (\pi K^*,\ K\rho)$ are used for the numerical calculation of the amplitudes $T_{P,V}$, $C_{P,V}$, $P_{P,V}$ and so on, except for $S_P^{(q,s,c)}$ and $S_V^{(q,s,c)}$ for which $\bar{B}_{u,d}(\bar{B}_s) \to \pi\omega/\phi\ (K\omega/\phi)$ and $\eta\rho\ (\eta K^*)$, respectively, are used. For $|\Delta S| = 1$ decays the processes $\bar{B}_{u,d}(\bar{B}_s) \to \pi K^*,\ K\rho\ (KK^*)$ are used to estimate $T'_{P,V}$, $C'_{P,V}$, $P'_{P,V}$ and so on, except for $S_P^{\prime(q,s,c)}$ and $S_V^{\prime(q,s,c)}$ for which $\bar{B}_{u,d}(\bar{B}_s) \to K\omega/\phi\ (\eta\omega/\phi)$ and $\eta K^*\ (\eta\phi)$, respectively, are used. The strong phases of the SU(3)$_{\rm F}$ amplitudes are generated from the flavor operators α_i^p and b_j^p. As shown in Eqs. (12)−(14), except the amplitudes $T^{(\prime)}$, $C^{(\prime)}$, $E^{(\prime)}$, $A^{(\prime)}$, $SE^{(\prime)}$ and $SA^{(\prime)}$, all the other amplitudes including penguin ones are the sum of two terms each of which is proportional to $\lambda_p^r \alpha_i^p$ or $\lambda_p^r b_j^p$ with $p = u, c$. Because the CKM factors λ_u^r and λ_c^r involve different weak phases from each other, to exhibit the strong phase of each amplitude in the tables, we shall use the approximations, $\alpha_{3,4({\rm EW})}^u \simeq \alpha_{3,4({\rm EW})}^c$ and $b_{3,4({\rm EW})}^u \simeq b_{3,4({\rm EW})}^c$, where the former (latter) relation holds roughly (very well) in QCDF. [5] Thus, for instance,

[5] In QCDF the value of α_i^c ($i = 3, 4, (3, {\rm EW}), (4, {\rm EW})$) differ from that of α_i^u by about $(25-30)\%$, while the

the QCD-penguin amplitude can be understood as $P^{(\prime)} \equiv -|P^{(\prime)}|e^{i\delta^{P^{(\prime)}}} e^{i\theta^{P^{(\prime)}}}$ with the strong phase $\delta^{P^{(\prime)}}$ and the weak phase $\theta^{P^{(\prime)}} = \arg(V_{tb}V^*_{td(s)})$.

From Tables XXV−XXVIII, hierarchies among the $\mathrm{SU(3)_F}$ amplitudes are numerically found as follows. For $\Delta S = 0$ $\bar{B}_{u,d}(\bar{B}_s) \to PP$ decays, the hierarchical relation is

$$\begin{aligned} |T_P| \;&>\; |C_P| > |P_P| \gtrsim |PE_P| > |E_P| > |S^{(s)}_P| \sim |S^{(q)}_P| \sim |P_{\mathrm{EW},\ P}| \sim |A_P| \sim |PA_P| \\ &>\; |P^C_{\mathrm{EW},\ P}| > |PE_{\mathrm{EW},\ P}| \sim |PA_{\mathrm{EW},\ P}| \sim |S^{(c)}_P| \ , \end{aligned} \tag{26}$$

and for $\bar{B}_{u,d}(\bar{B}_s) \to PV$,

$$\begin{aligned} |T_{P,V}| \;&>\; |C_{P,V}| > |PE_{P,V}| \gtrsim |P_{P,V}| \sim |E_{P,V}| > |P_{\mathrm{EW},\ P,V}| \gtrsim |A_{P,V}| \sim |S^{(s)}_{P,V}| \sim |S^{(q)}_{P,V}| \\ &\gtrsim\; |P^C_{\mathrm{EW},\ P,V}| > |PA_{P,V}| \gtrsim |PE_{\mathrm{EW},\ P,V}| \gtrsim |PA_{\mathrm{EW},\ P,V}| \sim |S^{(c)}_V| \ . \end{aligned} \tag{27}$$

Likewise, for $\Delta S = 1$ $\bar{B}_{u,d}(\bar{B}_s) \to PP$ decays, the hierarchical relation is found to be

$$\begin{aligned} |P'_P| \;&\gtrsim\; |PE'_P| > |T'_P| \gtrsim |P'_{\mathrm{EW},\ P}| \gtrsim |C'_P| \gtrsim |S'^{(s)}_P| \sim |S'^{(q)}_P| \sim |PA'_P| \\ &>\; |P^{C\prime}_{\mathrm{EW},\ P}| > |E'_P| > |A'_P| \sim |PE'_{\mathrm{EW},\ P}| \sim |PA'_{\mathrm{EW},\ P}| \gtrsim |S'^{(c)}_P| \ , \end{aligned} \tag{28}$$

and for $\bar{B}_{u,d}(\bar{B}_s) \to PV$,

$$\begin{aligned} &|PE'_{P,V}| \gtrsim |P'_{P,V}| > |T'_{P,V}| \gtrsim |P'_{\mathrm{EW},\ P,V}| > |C'_{P,V}| \sim |S'^{(s)}_{P,V}| \sim |S'^{(q)}_{P,V}| \gtrsim |P^{C\prime}_{\mathrm{EW},\ P,V}| \\ &> |PE'_{\mathrm{EW},\ V}| \gtrsim |PA'_{P,V}| \sim |E'_{P,V}| > |A'_{P,V}| > |PE'_{\mathrm{EW},\ P}| \sim |PA'_{\mathrm{EW},\ P,V}| \sim |S'^{(c)}_V| \ . \end{aligned} \tag{29}$$

Several remarks are in order:

1. It is well known that the penguin contributions are dominant in $|\Delta S| = 1$ decays due to the CKM enhancement $|V_{cs}V^*_{cb}| \approx |V_{ts}V^*_{tb}| \gg |V_{us}V^*_{ub}|$ and the large top quark mass. Especially, it is interesting to note that in addition to the QCD-penguin contributions $P'_{P,V}$, the QCD-penguin exchange ones $PE'_{P,V}$ are large for $\bar{B}_{u,d}(\bar{B}_s) \to PP$ and PV decays. Since the strong phase of $PE'_{P(V)}$ is comparable to that of $P'_{P(V)}$ in magnitude with the *same* sign (*i.e.*, $\delta^{PE\prime}_{P(V)} \sim \delta^{P\prime}_{P(V)}$), the effects from $PE'_{P(V)}$ and $P'_{P(V)}$ are strongly

value of b^c_i is the same as that of b^u_i. It should be emphasized that using Eqs. (12)−(14), one can compute both the magnitude and strong phase of each $\mathrm{SU(3)_F}$ amplitude without invoking these approximations on $\alpha^{u,c}_i$ and $b^{u,c}_i$. In our numerical analysis, we use these approximations only for expressing the strong phases as shown in Tables XXV−XXVIII. All the magnitudes of the amplitudes are obtained without using these approximations.

constructive to each other. It has been shown [24] that in order to accommodate the data including the branching fractions and CP asymmetries of those decays, the QCD-penguin exchange contributions ($PE'_{P,V} \propto b_3^p$) are important and play a crucial role. For example, for penguin-dominated $\bar{B}_{u,d} \to PP$ decays, the effects of the QCD-penguin exchange dictated by the values of ρ_A and ϕ_A paly a key role in resolving the problems of the smallness of predicted decay rates and of the wrong sign of the predicted direct CP asymmetry $A_{CP}(\pi^+K^-)$. Also, for $B_{u,d} \to K\rho$ and πK^* decays, the QCD-penguin exchange contributions will enhance the rates by $(15 \sim 100)\%$ for $K\rho$ modes and by a factor of $2 \sim 3$ for πK^* ones.

2. The $\mathrm{SU(3)_F}$-singlet contributions $S^{(\prime)}_{P,V}$ are involved in the decay modes including $\eta^{(\prime)}$, ω, ϕ in the final state, such as $\bar{B} \to \pi\eta^{(\prime)}$, $K\eta^{(\prime)}$, $\pi\omega/\phi$, $K\omega/\phi$, $\cdots$, etc. They are expected to be small because of the Okubo-Zweig-Iizuka (OZI) suppression rule which favors connected quark diagrams. Indeed they are found to be : $|S^{(\prime)}_P/P^{(\prime)}_P| \approx (10 \sim 24)\%$ for $\bar{B}_{u,d}(\bar{B}_s) \to PP$ and $|S^{(\prime)}_{P,V}/P^{(\prime)}_{P,V}| \approx (11 \sim 27)\%$ for $\bar{B}_{u,d}(\bar{B}_s) \to PV$. [6] In contrast, in the framework of generalized factorization, the $\mathrm{SU(3)_F}$-singlet contribution depend strongly on the parameter $\xi \equiv 1/N_c$ (N_c being the effective number of color) and could be large, particularly for $\bar{B}_{u,d} \to VV$ decays [16] : e.g., up to 77% of the dominant QCD-penguin contribution. In the flavor SU(3) analyses with a global fit of the $\mathrm{SU(3)_F}$ amplitudes to the data, a large effect from S'_P is also needed for explaining the large BFs of the $B \to \eta' K$ modes [30]: e.g., $|S'_P/P'_P| \approx 38\%$ [12].

   Among the two-body B decays, $B \to K\eta'$ has the largest branching fraction, of order 70×10^{-6}, while $\mathcal{B}(B \to \eta K)$ is only $(1 \sim 3) \times 10^{-6}$. This can be qualitatively understood as the interference between the $B \to K\eta_q$ amplitude induced by the $b \to sq\bar{q}$ penguin and the $B \to K\eta_s$ amplitude induced by $b \to ss\bar{s}$, which is constructive for $B \to K\eta'$ and destructive for $B \to \eta K$ [31]. This explains the large rate of the former and the suppression of the latter. As stressed in [21, 32], the observed large $B \to K\eta'$ rates are naturally explained in QCDF without invoking large flavor-singlet

[6] When the effects from $PE^{(\prime)}_{P,V}$ which are comparable to $P^{(\prime)}_{P,V}$ are taken into account, the ratio $|S^{(\prime)}_{P,V}/(P^{(\prime)}_{P,V} + PE^{(\prime)}_{P,V})|$ becomes $\lesssim 10\%$ for $\bar{B}_{u,d}(\bar{B}_s) \to PP$ and PV.

contributions.

3. In $\Delta S = 0$ decays, as expected, the tree contributions $T_{P,V}$ dominate and the color-suppressed tree amplitudes $C_{P,V}$ are larger than the penguin ones. Among the penguin contributions, the QCD-penguin ones $P_{P,V}$ and the QCD-penguin exchange ones $PE_{P,V}$ are comparable. Large strong phases in the decay amplitudes are needed to generate sizable direct CP violation in $\bar{B}$ decay processes. For tree-dominated $\bar{B}_{u,d}(\bar{B}_s) \to PP$ decays we have $C_P/T_P \approx 0.63\, e^{-i56^\circ}$ $(0.83\, e^{-i53^\circ})$ which is larger than the naive expectation of $C_P/T_P \sim 1/3$ in both magnitude and phase. Recall that a large complex color-suppressed tree topology C is needed to solve the rate deficit problems with $\pi^0\pi^0$ and $\pi^0\rho^0$ and give the correct sign for direct CP violation in the decays $K^-\pi^0$, $K^-\eta$, $\bar{K}^{*0}\eta$, $\pi^0\pi^0$ and $\pi^-\eta$ [24].

4. The W-exchange $E^{(\prime)}_{P,V}$, W-annihilation $A^{(\prime)}_{P,V}$ and QCD-penguin annihilation $PA^{(\prime)}_{P,V}$ contributions are small, as expected because of a helicity suppression factor of $f_B/m_B \approx 5\%$ arising from the smallness of the B meson wave function at the origin [15]; they are at most only a few % (or up to 12% in the case of PA'_A) of the dominant contributions $T_{P,V}$ or $P'_{P,V}$.

Finally let us compare the numerical values of the $\mathrm{SU}(3)_F$ amplitudes computed in QCDF with those obtained from global fits to charmless $\bar{B}_{u,d} \to PP$ and $\bar{B}_{u,d} \to PV$ decays. The ratios of the $\mathrm{SU}(3)_F$ amplitudes extracted from global fits to charmless $\bar{B}_{u,d} \to PP$ modes [12] are [7]

$$\begin{aligned}
&\left|\frac{C_P^{(\prime)}}{T_P^{(\prime)}}\right| = 0.67\ (0.67), \qquad && \left|\frac{P_P^{(\prime)}/\lambda_t^{d(s)}}{T_P^{(\prime)}/\lambda_u^{d(s)}}\right| = 0.17\ (0.14), \\
&\left|\frac{S_P^{(\prime)}/\lambda_t^{d(s)}}{T_P^{(\prime)}/\lambda_u^{d(s)}}\right| = 0.065\ (0.053), \qquad && \left|\frac{P_{\mathrm{EW},P}^{(\prime)}/\lambda_t^{d(s)}}{T_P^{(\prime)}/\lambda_u^{d(s)}}\right| = 0.020\ (0.016),
\end{aligned} \tag{30}$$

with $\lambda_q^r \equiv V_{qb}V_{qr}^*$ ($q = u, t$ and $r = d, s$), and the relative strong phases are

$$\begin{aligned}
&\delta_P^{C(\prime)} - \delta_P^{T(\prime)} = -68.3^\circ\ , \qquad && \delta_P^{P(\prime)} - \delta_P^{T(\prime)} = -15.9^\circ\ , \\
&\delta_P^{S(\prime)} - \delta_P^{T(\prime)} = -42.9^\circ\ , \qquad && \delta_P^{P_{\mathrm{EW}}(\prime)} - \delta_P^{T(\prime)} = -57.6^\circ\ .
\end{aligned} \tag{31}$$

[7] We only show the cases of "Scheme 4" in [12] for $\bar{B}_{u,d} \to PP$ and of "Scheme B2" in [13] for $\bar{B}_{u,d} \to PV$ below, since these cases take into account the largest set of SU(3) breaking effects among the four schemes presented in [12] and [13]. For comparison to our results, only the central values are shown.

Likewise, for charmless $\bar{B}_{u,d} \to PV$ modes, the ratios of the SU(3)$_F$ amplitudes extracted from global fits [13] are

$$\begin{aligned}
&\left|\frac{C_P^{(\prime)}}{T_P^{(\prime)}}\right| = 0.15\ (0.15), && \left|\frac{C_V^{(\prime)}}{T_V^{(\prime)}}\right| = 0.76\ (0.76),\\
&\left|\frac{P_P^{(\prime)}/\lambda_t^{d(s)}}{T_P^{(\prime)}/\lambda_u^{d(s)}}\right| = 0.11\ (0.11), && \left|\frac{P_V^{(\prime)}/\lambda_t^{d(s)}}{T_V^{(\prime)}/\lambda_u^{d(s)}}\right| = 0.056\ (0.046),\\
&\left|\frac{S_P^{(\prime)}/\lambda_t^{d(s)}}{T_P^{(\prime)}/\lambda_u^{d(s)}}\right| = 0.018\ (0.018), && \left|\frac{S_V^{(\prime)}/\lambda_t^{d(s)}}{T_V^{(\prime)}/\lambda_u^{d(s)}}\right| = 0.041\ (0.034),\\
&\left|\frac{P_{\rm EW,P}^{(\prime)}/\lambda_t^{d(s)}}{T_P^{(\prime)}/\lambda_u^{d(s)}}\right| = 0.039\ (0.039), && \left|\frac{P_{\rm EW,V}^{(\prime)}/\lambda_t^{d(s)}}{T_V^{(\prime)}/\lambda_u^{d(s)}}\right| = 0.074\ (0.061),
\end{aligned} \tag{32}$$

and the relative strong phases are

$$\begin{aligned}
&\delta_P^{C(\prime)} - \delta_P^{T(\prime)} = 149.0^\circ\ , && \delta_V^{T(\prime)} - \delta_P^{T(\prime)} = 0.6^\circ\ , && \delta_V^{C(\prime)} - \delta_P^{T(\prime)} = -75.9^\circ\ ,\\
&\delta_P^{P(\prime)} - \delta_P^{T(\prime)} = -2.6^\circ\ , && \delta_V^{P(\prime)} - \delta_P^{T(\prime)} = 172.5^\circ\ ,\\
&\delta_P^{S(\prime)} - \delta_P^{T(\prime)} = -139.8^\circ\ , && \delta_V^{S(\prime)} - \delta_P^{T(\prime)} = -47.7^\circ\ ,\\
&\delta_P^{P_{\rm EW}(\prime)} - \delta_P^{T(\prime)} = 59.0^\circ\ , && \delta_V^{P_{\rm EW}(\prime)} - \delta_P^{T(\prime)} = -111.0^\circ\ .
\end{aligned} \tag{33}$$

In the above the numerical values outside (inside) parentheses correspond to $\Delta S = 0$ ($|\Delta S| = 1$) decays. In the case of $\bar{B}_{u,d} \to PP$ with $|\Delta S| = 1$, the *primed* amplitudes were obtained by including the SU(3) breaking factor f_K/f_π for both $|T'_P|$ and $|C'_P|$ and a universal SU(3) breaking factor $\xi = 1.04$ for all the amplitudes except $P'_{\rm EW,P}$. But, in $\bar{B}_{u,d} \to PV$, the *primed* amplitudes were extracted by imposing partial SU(3) breaking factors on T and C only: *i.e.*, including f_{K^*}/f_ρ for $|T'_P|$ and $|C'_P|$, and f_K/f_π for $|T'_V|$ and $|C'_V|$. Also, for both $\bar{B}_{u,d} \to PP$ and PV, the top penguin dominance was assumed, which is equivalent to the assumption that $\alpha^u_{3,4({\rm EW})} \simeq \alpha^c_{3,4({\rm EW})}$ in QCDF. For the strong phases, exact flavor SU(3) symmetry was assumed in the fits so that $\delta_P^T = \delta_P^{T\prime}$, $\delta_P^C = \delta_P^{C\prime}$, etc. In $\bar{B}_{u,d} \to PV$, all the relative strong phases were found relative to the strong phase of T_P (*i.e.*, δ_P^T).

On the other hand, from Table XXV, the ratios of the SU(3)$_F$ amplitudes for $\bar{B}_{u,d} \to PP$ are given by

$$\begin{aligned}
&\left|\frac{C_P^{(\prime)}}{T_P^{(\prime)}}\right| = 0.63\ (0.64), && \left|\frac{P_P^{(\prime)}/\lambda_t^{d(s)}}{T_P^{(\prime)}/\lambda_u^{d(s)}}\right| = 0.091\ (0.097),\\
&\left|\frac{S_P^{(\prime)(q)}/\lambda_t^{d(s)}}{T_P^{(\prime)}/\lambda_u^{d(s)}}\right| = 0.014\ (0.012), && \left|\frac{P_{\rm EW,P}^{(\prime)}/\lambda_t^{d(s)}}{T_P^{(\prime)}/\lambda_u^{d(s)}}\right| = 0.013\ (0.016),
\end{aligned}$$

$$\left|\frac{PE_P^{(\prime)}/\lambda_t^{d(s)}}{T_P^{(\prime)}/\lambda_u^{d(s)})}\right| = 0.061\ (0.060), \tag{34}$$

and the relative strong phases are

$$\begin{aligned}
&\delta_P^{C(\prime)} - \delta_P^{T(\prime)} = -55.7^\circ\ (-57.5^\circ)\ , \qquad && \delta_P^{P(\prime)} - \delta_P^{T(\prime)} = -158.6^\circ\ (-158.3^\circ)\ , \\
&\delta_P^{S^{(\prime)(q)}} - \delta_P^{T(\prime)} = 158.2^\circ\ (149.4^\circ)\ , \qquad && \delta_P^{P_{\rm EW}(\prime)} - \delta_P^{T(\prime)} = -179.8^\circ\ (-179.8^\circ)\ , \\
&\delta_P^{PE(\prime)} - \delta_P^{T(\prime)} = -147.1^\circ\ (-147.1^\circ)\ .
\end{aligned} \tag{35}$$

Likewise, for $\bar{B}_{u,d} \to PV$, we obtain

$$\begin{aligned}
&\left|\frac{C_P^{(\prime)}}{T_P^{(\prime)}}\right| = 0.30\ (0.35), && \left|\frac{C_V^{(\prime)}}{T_V^{(\prime)}}\right| = 0.39\ (0.33), \\
&\left|\frac{P_P^{(\prime)}/\lambda_t^{d(s)}}{T_P^{(\prime)}/\lambda_u^{d(s)}}\right| = 0.030\ (0.036), && \left|\frac{P_V^{(\prime)}/\lambda_t^{d(s)}}{T_V^{(\prime)}/\lambda_u^{d(s)}}\right| = 0.041\ (0.039), \\
&\left|\frac{S_P^{(\prime)}/\lambda_t^{d(s)}}{T_P^{(\prime)}/\lambda_u^{d(s)}}\right| = 0.005\ (0.006), && \left|\frac{S_V^{(\prime)}/\lambda_t^{d(s)}}{T_V^{(\prime)}/\lambda_u^{d(s)}}\right| = 0.010\ (0.007), \\
&\left|\frac{P_{{\rm EW},P}^{(\prime)}/\lambda_t^{d(s)}}{T_P^{(\prime)}/\lambda_u^{d(s)}}\right| = 0.014\ (0.019), && \left|\frac{P_{{\rm EW},V}^{(\prime)}/\lambda_t^{d(s)}}{T_V^{(\prime)}/\lambda_u^{d(s)}}\right| = 0.013\ (0.014), \\
&\left|\frac{PE_P^{(\prime)}/\lambda_t^{d(s)}}{T_P^{(\prime)}/\lambda_u^{d(s)}}\right| = 0.037\ (0.040), && \left|\frac{PE_V^{(\prime)}/\lambda_t^{d(s)}}{T_V^{(\prime)}/\lambda_u^{d(s)}}\right| = 0.051\ (0.049),
\end{aligned} \tag{36}$$

and the relative strong phases are

$$\begin{aligned}
&\delta_P^{C(\prime)} - \delta_P^{T(\prime)} = -16.8^\circ\ (-19.8^\circ)\ , \qquad && \delta_V^{C(\prime)} - \delta_P^{T(\prime)} = -52.5^\circ\ (-56.2^\circ)\ , \\
&\delta_P^{P(\prime)} - \delta_P^{T(\prime)} = -145.5^\circ\ (-145.2^\circ)\ , \qquad && \delta_V^{P(\prime)} - \delta_P^{T(\prime)} = 7.6^\circ\ (7.1^\circ)\ , \\
&\delta_P^{S(\prime)} - \delta_P^{T(\prime)} = -5.5^\circ\ (-6.4^\circ)\ , \qquad && \delta_V^{S(\prime)} - \delta_P^{T(\prime)} = 150.7^\circ\ (133.4^\circ)\ , \\
&\delta_P^{P_{\rm EW}(\prime)} - \delta_P^{T(\prime)} = 179.8^\circ\ (179.8^\circ)\ , \qquad && \delta_V^{P_{\rm EW}(\prime)} - \delta_P^{T(\prime)} = -179.7^\circ\ (-179.7^\circ)\ , \\
&\delta_P^{PE(\prime)} - \delta_P^{T(\prime)} = -124.4^\circ\ (-125.0^\circ)\ , \qquad && \delta_V^{PE(\prime)} - \delta_P^{T(\prime)} = 4.5^\circ\ (4.2^\circ)\ ,
\end{aligned} \tag{37}$$

where the numerical values outside (inside) parentheses correspond to $\Delta S = 0$ ($|\Delta S| = 1$) decays. In our case, $\delta_P^T = \delta_V^T = \delta_P^{T\prime} = \delta_V^{T\prime}$.

In comparison of Eqs. (30)−(33) [*"fitting case"*] with Eqs. (34)−(37) [*"QCDF case"*], it is found that the values of $|C_P^{(\prime)}/T_P^{(\prime)}|$ for $\bar{B}_{u,d} \to PP$ in the *fitting case* are very similar to those of our *QCDF case*: both results show the large magnitudes of $C_P^{(\prime)}$ together with large strong phases, as discussed in the above "*remark* 3". But, for $\bar{B}_{u,d} \to PV$, the values

of $|C^{(\prime)}_{P,V}/T^{(\prime)}_{P,V}|$ from both cases are different: in the *fitting case*, the ratios $|C^{(\prime)}_V/T^{(\prime)}_V|$ are significantly larger than $|C^{(\prime)}_P/T^{(\prime)}_P|$, though the values of $|C^{(\prime)}_P|$ include large errors in [13], while in the *QCDF case* $|C^{(\prime)}_V/T^{(\prime)}_V| \sim |C^{(\prime)}_P/T^{(\prime)}_P|$. For the penguin amplitudes, the results from both cases are also different. The values of $|(P^{(\prime)}_P/\lambda_t^{d(s)})/(T^{(\prime)}_P/\lambda_u^{d(s)})|$ for both $\bar{B}_{u,d} \to PP$ and PV in the *fitting case* are larger than those in the *QCDF case*. In the latter case, the effects from $PE^{(\prime)}_P$ are comparable to and contribute constructively to those of $P^{(\prime)}_P$, as discussed in the above "*remark* 1". Interestingly it is found that the combined effects from $P^{(\prime)}_P$ and $PE^{(\prime)}_P$ obtained in the *QCDF case* are comparable to that of $P^{(\prime)}_P$ determined in the *fitting case*. In contrast, the combined effects from $P^{(\prime)}_V$ and $PE^{(\prime)}_V$ found in the *QCDF case* are (roughly two times) larger than that of $P^{(\prime)}_P$ obtained in the *fitting case*. Also, for $\bar{B}_{u,d} \to PV$ decays, the ratio $|(P^{(\prime)}_P/\lambda_t^{d(s)})/(T^{(\prime)}_P/\lambda_u^{d(s)})| \sim |(P^{(\prime)}_V/\lambda_t^{d(s)})/(T^{(\prime)}_V/\lambda_u^{d(s)})|$ in the *QCDF case*, while $|(P^{(\prime)}_P/\lambda_t^{d(s)})/(T^{(\prime)}_P/\lambda_u^{d(s)})| \sim 2|(P^{(\prime)}_V/\lambda_t^{d(s)})/(T^{(\prime)}_V/\lambda_u^{d(s)})|$ in the *fitting case*. For the $\mathrm{SU(3)_F}$-singlet contributions, as discussed in the above "*remark* 2", $S^{(\prime)}_{P,V}$ obtained in the *fitting case* are much larger than those found in the *QCDF case*: e.g., for $\bar{B}_{u,d} \to PV$, the ratio $|S^{(\prime)}_V/P^{(\prime)}_V| \approx 73\%$ in the *fitting case*, in contrast to $|S^{(\prime)}_V/(P^{(\prime)}_V + PE^{(\prime)}_V)| \lesssim 10\%$ [or $|S^{(\prime)}_V/P^{(\prime)}_V| \approx (18-24)\%$] in the *QCDF case*.

B. Estimates of decay amplitudes, $\mathrm{SU(3)_F}$ breaking effects and $\mathrm{SU(3)_F}$ relations

Using Tables XXV−XXVIII, one can easily estimate the decay amplitudes of $\bar{B}_{u,d}(\bar{B}_s) \to PP,\ PV$ numerically. For example, the decay amplitude of $B^- \to \pi^-\pi^0$ is obtained as

$$\begin{aligned}\sqrt{2}\mathcal{A}_{B^-\to\pi^-\pi^0} &= T_\pi + C_\pi + P_{\mathrm{EW},\pi} + P^C_{\mathrm{EW},\pi} \\ &= (1.52 - i\ 24.94) \times 10^{-9}\ \mathrm{GeV}\ ,\end{aligned} \tag{38}$$

and the decay amplitude of $B^- \to \pi^-\bar{K}^0$ given in Eq. (9) is estimated as

$$\mathcal{A}_{B^-\to\pi^-\bar{K}^0} = (-49.71 - i\ 24.77) \times 10^{-9}\ \mathrm{GeV}\ . \tag{39}$$

Likewise, the decay amplitude of $\bar{B}_s \to K^0\pi^0$ is found to be

$$\begin{aligned}\mathcal{A}_{\bar{B}_s\to K^0\pi^0} &= C_K - P_K + P_{\mathrm{EW},K} + \frac{1}{3}P^C_{\mathrm{EW},K} - PE_K + \frac{1}{3}PE_{\mathrm{EW},K} \\ &= (-16.32 - i\ 17.91) \times 10^{-9}\ \mathrm{GeV}\ ,\end{aligned} \tag{40}$$

and the decay amplitude of $\bar{B}_s \to K^+ K^{*-}$ is given by

$$\begin{aligned}\mathcal{A}_{\bar{B}_s\to K^+K^{*-}} &= T'_K + P'_K + \frac{2}{3}P^{C\prime}_{\rm EW,K} + E'_{K^*} + PE'_K + PA'_K + PA'_{K^*} \\ &\quad -\frac{1}{3}PE'_{\rm EW,K} - \frac{1}{3}PA'_{\rm EW,K} + \frac{2}{3}PE'_{\rm EW,K^*} \\ &= (-30.20 - i\ 4.97)\times 10^{-9}\ {\rm GeV}\ . \end{aligned} \tag{41}$$

In the above, the color-suppressed and color-favored tree amplitudes are, for example, $C_K \equiv |C_K|\ e^{i\left(\delta^C_K+\theta^C\right)}$ and $T'_K \equiv |T'_K|\ e^{i\left(\delta^{T\prime}_K+\theta^{T\prime}\right)}$, respectively, with the strong phases δ^C_K and $\delta^{T\prime}_K$ and the weak phases $\theta^C = \arg(V_{ub}V^*_{ud})$ and $\theta^{T\prime} = \arg(V_{ub}V^*_{us})$. The QCD- and EW-penguin and weak annihilation amplitudes have the similar form, such as $P^{(\prime)}_K \equiv |P^{(\prime)}_K|\ e^{i\left(\delta^{P^{(\prime)}}_K+\theta^{P^{(\prime)}}\right)}$ and $E_{K^*} \equiv |E'_{K^*}|\ e^{i\left(\delta^{E\prime}_{K^*}+\theta^{E\prime}\right)}$, etc, where the strong phases $\delta^P_K \neq \delta^{P\prime}_K \neq \delta^{E\prime}_{K^*}$ in general and the weak phases $\theta^P = \arg(-V_{tb}V^*_{td})$ and $\theta^{P\prime} = \theta^{E\prime} = \arg(-V_{tb}V^*_{ts})$. By using Eqs. (38)−(41), and noting that each $\mathrm{SU(3)_F}$ amplitude and its CP-conjugate one are the same except for having the weak phase with opposite sign to each other (e.g., the CP-conjugate amplitude to C_K is $|C_K|\ e^{i\left(\delta^C_K-\theta^C\right)}$), the estimation of direct CP asymmetries as well as the decay rates can be easily obtained.

The $\mathrm{SU(3)_F}$ breaking effects in the amplitudes arise from the decay constants, masses of the mesons and the form factors in addition to the CKM matrix elements. For example, taking into account the effects of $\mathrm{SU(3)_F}$ breaking in $\bar{B}_{u,d} \to PP$, the ratio of T'_P and T_P is estimated by $|T'_P/T_P| \approx [|V_{us}|\ f_K(m_B^2 - m_K^2)F_0^{BK}]/[|V_{ud}|\ f_\pi(m_B^2 - m_\pi^2)F_0^{B\pi}]$. From Tables XXV−XXVIII, the numerical estimates of the $\mathrm{SU(3)_F}$ breaking effects in the amplitudes can be obtained. For both $\bar{B}_{u,d}(\bar{B}_s) \to PP$ decays with $\Delta S = 0$ and $|\Delta S| = 1$,

$$\begin{aligned} &\left|\frac{V_{ud}\ T'_P}{V_{us}\ T_P}\right| = 1.22\ (1.21), \quad \left|\frac{V_{ud}\ C'_P}{V_{us}\ C_P}\right| = 1.25\ (1.26), \\ &\left|\frac{V_{td}\ P'_P}{V_{ts}\ P_P}\right| = 1.18\ (1.18), \quad \left|\frac{V_{td}\ PE'_P}{V_{ts}\ PE_P}\right| = 1.19\ (1.19). \end{aligned} \tag{42}$$

Likewise, for $\bar{B}_{u,d} \to PV$ decays,

$$\begin{aligned} &\left|\frac{V_{ud}\ T'_{P(V)}}{V_{us}\ T_{P(V)}}\right| = 1.02\ (1.23), \quad \left|\frac{V_{ud}\ C'_{P(V)}}{V_{us}\ C_{P(V)}}\right| = 1.19\ (1.02), \\ &\left|\frac{V_{td}\ P'_{P(V)}}{V_{ts}\ P_{P(V)}}\right| = 1.07\ (1.12), \quad \left|\frac{V_{td}\ PE'_{P(V)}}{V_{ts}\ PE_{P(V)}}\right| = 1.10\ (1.18), \end{aligned} \tag{43}$$

and for $\bar{B}_s \to PV$ decays,

$$\left|\frac{V_{ud}\ T'_{P(V)}}{V_{us}\ T_{P(V)}}\right| = 1.02\ (1.22), \quad \left|\frac{V_{ud}\ C'_{P(V)}}{V_{us}\ C_{P(V)}}\right| = 1.00\ (1.28),$$

$$\left|\frac{V_{td}\ P'_{P(V)}}{V_{ts}\ P_{P(V)}}\right| = 1.07\ (1.15), \qquad \left|\frac{V_{td}\ PE'_{P(V)}}{V_{ts}\ PE_{P(V)}}\right| = 1.11\ (1.18). \tag{44}$$

In the above, we have factored out the relevant CKM matrix element from each $\mathrm{SU(3)_F}$ amplitude. The results show that the $\mathrm{SU(3)_F}$ breaking is up to 28% for the tree and color-suppressed tree amplitudes, and 19% for the QCD-penguin and QCD-penguin exchange amplitudes.

In Refs. [15, 16], a number of $\mathrm{SU(3)_F}$ linear relations among various decay amplitudes were presented. These relations were suggested to be used in testing various assumptions made in the $\mathrm{SU(3)_F}$ analysis and extracting CP phases and strong final-state phases and so on. In the previous studies, certain diagrams, such as the QCD-penguin exchange PE' and the EW-penguin exchange $PE'_{\rm EW}$, were ignored. As we have discussed in the previous subsection, the contribution from the PE' diagram turns out to be important in $|\Delta S| = 1$ decay processes. Because of its topology, the QCD-penguin exchange amplitude PE' always appears in the decay amplitude together with the QCD-penguin one P'. Thus, all the $\mathrm{SU(3)_F}$ linear relations obtained in [15, 16] still hold after replacing P' by $(P' + PE')$. However, due to this replacement, the relevant strong phase of P' should be changed as follows:

$$P' = |P'|e^{i\delta^{P'}}e^{i\theta^{P'}} \quad \to \quad P' + PE' = |P'|e^{i\delta^{P'}}e^{i\theta^{P'}} + |PE'|e^{i\delta^{PE'}}e^{i\theta^{PE'}} \equiv |\tilde{P}'|e^{i\delta^{\tilde{P}'}}e^{i\theta^{\tilde{P}'}}, \tag{45}$$

where the weak phases $\theta^{P'} = \theta^{PE'} = \theta^{\tilde{P}'}$ under the assumption that the top quark dominates the penguin amplitudes in the relevant processes. Apparently, the strong phase $\delta^{\tilde{P}'}$ is generally not the same as $\delta^{P'}$, although they differ not much because roughly $|P'| \sim |PE'|$ and $\delta^{P'} \sim \delta^{PE'}$, as shown in Eqs. (34)$-$(37). In fact, $\delta^{\tilde{P}'}$ arises from the different flavor operators $\alpha_4^{u,c}$ and $b_3^{u,c}$ in QCDF.

For completeness, we present some useful $\mathrm{SU(3)_F}$ relations among the decay amplitudes of $\bar{B}_d(\bar{B}_s) \to PV$ which are not given in [15]. ¿From Tables VII$-$XII and XIX$-$XXIV, we find

$$\begin{aligned}
\mathcal{A}_{\bar{B}_s\to\pi^-K^{*+}} &= T_{K^*} + P_{K^*} + \frac{2}{3}P^C_{{\rm EW},K^*} + PE_{K^*} - \frac{1}{3}PE_{{\rm EW},K^*}\ , \\
\mathcal{A}_{\bar{B}_d\to\pi^-\rho^+} &= T_\rho + P_\rho + \frac{2}{3}P^C_{{\rm EW},\rho} + E_\pi + PE_\rho + PA_\pi + PA_\rho - \frac{1}{3}PE_{{\rm EW},\rho} \\
&\quad + \frac{2}{3}PA_{{\rm EW},\pi} - \frac{1}{3}PA_{{\rm EW},\rho}\ , \\
\mathcal{A}_{\bar{B}_s\to K^+\rho^-} &= T_K + P_K + \frac{2}{3}P^C_{{\rm EW},K} + PE_K - \frac{1}{3}PE_{{\rm EW},K}\ ,
\end{aligned}$$

$$
\begin{aligned}
\mathcal{A}_{\bar{B}_d\to\pi^+\rho^-} &= T_\pi + P_\pi + \frac{2}{3}P^C_{\rm EW,\pi} + E_\rho + PE_\pi + PA_\rho + PA_\pi - \frac{1}{3}PE_{\rm EW,\pi} \\
&\quad + \frac{2}{3}PA_{\rm EW,\rho} - \frac{1}{3}PA_{\rm EW,\pi} \ , \\
\mathcal{A}_{\bar{B}_s\to K^-K^{*+}} &= T'_{K^*} + P'_{K^*} + \frac{2}{3}P^{C\prime}_{\rm EW,K^*} + E'_K + PE'_{K^*} + PA'_{K^*} + PA'_K \\
&\quad - \frac{1}{3}PE'_{\rm EW,K^*} - \frac{1}{3}PA'_{\rm EW,K^*} + \frac{2}{3}PA'_{\rm EW,K} \ , \\
\mathcal{A}_{\bar{B}_d\to K^-\rho^+} &= T'_\rho + P'_\rho + \frac{2}{3}P^{C\prime}_{\rm EW,\rho} + PE'_\rho - \frac{1}{3}PE'_{\rm EW,\rho} \ , \\
\mathcal{A}_{\bar{B}_d\to\pi^+K^{*-}} &= T'_\pi + P'_\pi + \frac{2}{3}P^{C\prime}_{\rm EW,\pi} + PE'_\pi - \frac{1}{3}PE'_{\rm EW,\pi} \ .
\end{aligned}
\tag{46}
$$

Also, from Tables XXVI and XXVIII, we see that $|E^{(\prime)}_{\pi,\rho,K^{(*)}}|, |PA^{(\prime)}_{\pi,\rho,K^{(*)}}|, |PA^{(\prime)}_{\rm EW,\pi,\rho,K^{(*)}}| \ll |T^{(\prime)}_{\pi,\rho,K^{(*)}}|$ and the dominant contributions $|T_{K^*(K)}| \simeq |T_{\rho(\pi)}|$, $|P'_{K^*(K)}| \simeq |P'_{\rho(\pi)}|$ and $|PE'_{K^*(K)}| \simeq |PE'_{\rho(\pi)}|$. Thus, it is expected from Eqs. (41) and (46) that

$$
\begin{aligned}
&\mathcal{A}_{\bar{B}_s\to\pi^-K^{*+}} \simeq \mathcal{A}_{\bar{B}_d\to\pi^-\rho^+} \ , && \mathcal{A}_{\bar{B}_s\to K^+\rho^-} \simeq \mathcal{A}_{\bar{B}_d\to\pi^+\rho^-} \ , \\
&\mathcal{A}_{\bar{B}_s\to K^-K^{*+}} \simeq \mathcal{A}_{\bar{B}_d\to K^-\rho^+} \ , && \mathcal{A}_{\bar{B}_s\to K^+K^{*-}} \simeq \mathcal{A}_{\bar{B}_d\to\pi^+K^{*-}} \ .
\end{aligned}
\tag{47}
$$

Consequently, we obtain the relations for the BFs and the direct CP asymmetries :

$$
\begin{aligned}
&\mathcal{B}(\bar{B}_s\to\pi^-K^{*+}) \simeq \mathcal{B}(\bar{B}_d\to\pi^-\rho^+) \ , && \mathcal{B}(\bar{B}_s\to K^+\rho^-) \simeq \mathcal{B}(\bar{B}_d\to\pi^+\rho^-) \ , \\
&\mathcal{B}(\bar{B}_s\to K^-K^{*+}) \simeq \mathcal{B}(\bar{B}_d\to K^-\rho^+) \ , && \mathcal{B}(\bar{B}_s\to K^+K^{*-}) \simeq \mathcal{B}(\bar{B}_d\to\pi^+K^{*-}) \ , \\
&A_{CP}(\bar{B}_s\to\pi^-K^{*+}) \simeq A_{CP}(\bar{B}_d\to\pi^-\rho^+) \ , && A_{CP}(\bar{B}_s\to K^+\rho^-) \simeq A_{CP}(\bar{B}_d\to\pi^+\rho^-) \ , \\
&A_{CP}(\bar{B}_s\to K^-K^{*+}) \simeq A_{CP}(\bar{B}_d\to K^-\rho^+) \ , && A_{CP}(\bar{B}_s\to K^+K^{*-}) \simeq A_{CP}(\bar{B}_d\to\pi^+K^{*-}) \ .
\end{aligned}
\tag{48}
$$

Numerically the above $\mathrm{SU(3)_F}$ relations are generally respected [24].

IV. CONCLUSION

Based on flavor SU(3) symmetry, we have presented a model-independent analysis of $\bar{B}_{u,d}(\bar{B}_s) \to PP,\ PV$ decays. Based on the topological diagrams, all the decay amplitudes of interest have been expressed in terms of the the $\mathrm{SU(3)_F}$ amplitudes. In order to bridge the topological-diagram approach (or the flavor SU(3) analysis) and the QCDF approach, we have explicitly shown how to translate each $\mathrm{SU(3)_F}$ amplitude involved in these decay modes into the corresponding terms in the framework of QCDF. This is practically a way to easily find the rather *sophisticated* results of the relevant decay amplitudes calculated in QCDF by

taking into account the simpler and more *intuitive* topological diagrams of relevance. For further quantitative discussions, we have numerically computed each $\mathrm{SU(3)_F}$ amplitude in QCDF and shown its magnitude and strong phase.

In our analysis, we have included the presumably subleading diagrams, such as the QCD- and EW-penguin exchange ones (PE and $PE_{\rm EW}$) and flavor-singlet weak annihilation ones (SE, SA, SPE, SPA, $SPE_{\rm EW}$, $SPA_{\rm EW}$). Among them, the contribution from the QCD-penguin exchange diagram plays a crucial role in understanding the branching fractions and direct CP asymmetries for penguin-dominant decays with $|\Delta S| = 1$, such as $\bar{B}_{u,d} \to \pi^+ K^-$, $K\rho$, πK^* decays. Numerically the $\mathrm{SU(3)_F}$-singlet amplitudes $S^{(\prime)}_{P,V}$ involved in $\bar{B}_{u,d}(\bar{B}_s) \to \pi\eta^{(\prime)}$, $K\eta^{(\prime)}$, $\pi\,\omega/\phi$, $K\,\omega/\phi$, etc, are found to be small as expected from the OZI suppression rule. On the other hand, the color-suppressed tree amplitude C is found to be large and complex : e.g., for tree-dominated $\bar{B}_{u,d}(\bar{B}_s) \to PP$ decays, $C_P/T_P \approx 0.63\, e^{-i56^\circ}$ $(0.83\, e^{-i53^\circ})$ which is larger than the naive expectation of $C_P/T_P \sim 1/3$ in phase and magnitude. This large complex C is needed to understand the experimental data for the branching fractions of $\bar{B}_d \to \pi^0\pi^0$, $\pi^0\rho^0$ and the direct CP asymmetries in $\bar{B}_{u,d} \to K^-\pi^0$, $K^-\eta$, $\bar{K}^{*0}\eta$, $\pi^0\pi^0$, $\pi^-\eta$ modes. We have also compared our results with those obtained from global fits to $\bar{B}_{u,d} \to PP,\ PV$ decays. Certain results, such as the effects of $C^{(\prime)}_P$ for $\bar{B}_{u,d} \to PP$, are consistent with each other, but some other results, such as the contributions of $P^{(\prime)}_{P,V}$ and $S^{(\prime)}_{P,V}$ for $\bar{B}_{u,d} \to PP,\ PV$, are different from each other. These differences stem mainly from the different ways of explaining the current data of $\bar{B}_{u,d} \to PP, PV$ in these two approaches, depending on which $\mathrm{SU(3)_F}$ amplitudes become more important in a particular mode.

As an example of the applications, we have discussed the $\mathrm{SU(3)_F}$ breaking effects. Our results show that the $\mathrm{SU(3)_F}$ breaking is up to 28% for the tree and color-suppressed tree amplitudes and 19% for the QCD-penguin and QCD-penguin exchange ones. Using the $\mathrm{SU(3)_F}$ amplitudes, we have also derived some useful relations among the decay amplitudes of $\bar{B}_s \to PV$ and $\bar{B}_d \to PV$. These $\mathrm{SU(3)_F}$ relations are expected to be tested in future experiments such as the upcoming LHCb one.

Acknowledgments

This work was supported in part by the National Science Council of R.O.C. under Grants Numbers: NSC-97-2112-M-001-004-MY3 and NSC-99-2811-M-001-038.

TABLE I: Coefficients of $\mathrm{SU(3)_F}$ amplitudes in $\bar{B} \to P_1 P_2$ ($\Delta S = 0$).

$\bar{B} \to P_1 P_2$	factor	$T^{(\zeta)}_{P_1\ [P_2]}$	$C^{(\zeta)}_{P_1\ [P_2]}$	$S^{(\zeta)}_{P_1\ [P_2]}$	$P^{(\zeta)}_{P_1\ [P_2]}$	$P^{(\zeta)}_{\mathrm{EW},\ P_1\ [P_2]}$	$P^{C,\ (\zeta)}_{\mathrm{EW},\ P_1\ [P_2]}$
$B^- \to \pi^- \pi^0$	$\frac{1}{\sqrt{2}}$	0	1	0	-1	1	$\frac{1}{3}$
		$[1]$	$[0]$	$[0]$	$[1]$	$[0]$	$[\frac{2}{3}]$
$\bar{B}^0 \to \pi^- \pi^+$	1	1	0	0	1	0	$\frac{2}{3}$
		$[0]$	$[0]$	$[0]$	$[0]$	$[0]$	$[0]$
$\bar{B}^0 \to \pi^0 \pi^0$	$-\frac{1}{2}$	0	1	0	-1	1	$\frac{1}{3}$
		$[0]$	$[1]$	$[0]$	$[-1]$	$[1]$	$[\frac{1}{3}]$
$B^- \to K^- K^0$	1	0	0	0	1	0	$-\frac{1}{3}$
		$[0]$	$[0]$	$[0]$	$[0]$	$[0]$	$[0]$
$\bar{B}^0 \to K^- K^+$	1	0	0	0	0	0	0
		$[0]$	$[0]$	$[0]$	$[0]$	$[0]$	$[0]$
$\bar{B}^0 \to \bar{K}^0 K^0$	1	0	0	0	1	0	$-\frac{1}{3}$
		$[0]$	$[0]$	$[0]$	$[0]$	$[0]$	$[0]$
$B^- \to \pi^- \eta^{(\prime)}$	$\frac{1}{\sqrt{2}}$	0	$1(q) + \sqrt{2}(c)$	$2(q) + \sqrt{2}(s) + \sqrt{2}(c)$	$1(q)$	$\frac{1}{3}(q) - \frac{\sqrt{2}}{3}(s)$	$-\frac{1}{3}(q)$
		$[1(q)]$	$[0]$	$[0]$	$[1(q)]$	$[0]$	$[\frac{2}{3}(q)]$
$\bar{B}^0 \to \pi^0 \eta^{(\prime)}$	$-\frac{1}{2}$	0	$1(q) + \sqrt{2}(c)$	$2(q) + \sqrt{2}(s) + \sqrt{2}(c)$	$1(q)$	$\frac{1}{3}(q) - \frac{\sqrt{2}}{3}(s)$	$-\frac{1}{3}(q)$
		$[0]$	$[-1(q)]$	$[0]$	$[1(q)]$	$[-1(q)]$	$[-\frac{1}{3}(q)]$
$\bar{B}^0 \to \eta^{(\prime)} \eta^{(\prime)}$	$\frac{1}{2}$	0	$1(q,q)$	$2(q,q) + \sqrt{2}(q,s)$	$1(q,q)$	$\frac{1}{3}(q,q)$	$-\frac{1}{3}(q,q)$
			$+\sqrt{2}(q,c)$	$+\sqrt{2}(q,c)$		$-\frac{\sqrt{2}}{3}(q,s)$	
		$[0]$	$[1(q,q)$	$[2(q,q) + \sqrt{2}(q,s)$	$[1(q,q)]$	$[\frac{1}{3}(q,q)$	$[-\frac{1}{3}(q,q)]$
			$+\sqrt{2}(q,c)]$	$+\sqrt{2}(q,c)]$		$-\frac{\sqrt{2}}{3}(q,s)]$	

TABLE II: (*Continued from Table I*) Weak annihilation contributions.

$\bar{B} \to P_1 P_2$	factor	$E^{(\zeta)}_{P_1\ [P_2]}$	$A^{(\zeta)}_{P_1\ [P_2]}$	$PE^{(\zeta)}_{P_1\ [P_2]}$	$PA^{(\zeta)}_{P_1\ [P_2]}$	$PE^{(\zeta)}_{\mathrm{EW},\ P_1\ [P_2]}$	$PA^{(\zeta)}_{\mathrm{EW},\ P_1\ [P_2]}$
$B^- \to \pi^-\pi^0$	$\frac{1}{\sqrt{2}}$	0	-1	-1	0	$-\frac{2}{3}$	0
		$[0]$	$[1]$	$[1]$	$[0]$	$[\frac{2}{3}]$	$[0]$
$\bar{B}^0 \to \pi^-\pi^+$	1	0	0	1	1	$-\frac{1}{3}$	$-\frac{1}{3}$
		$[1]$	$[0]$	$[0]$	$[1]$	$[0]$	$[\frac{2}{3}]$
$\bar{B}^0 \to \pi^0\pi^0$	$-\frac{1}{2}$	-1	0	-1	-2	$\frac{1}{3}$	$-\frac{1}{3}$
		$[-1]$	$[0]$	$[-1]$	$[-2]$	$[\frac{1}{3}]$	$[-\frac{1}{3}]$
$B^- \to K^-K^0$	1	0	1	1	0	$\frac{2}{3}$	0
		$[0]$	$[0]$	$[0]$	$[0]$	$[0]$	$[0]$
$\bar{B}^0 \to K^-K^+$	1	1	0	0	1	0	$\frac{2}{3}$
		$[0]$	$[0]$	$[0]$	$[1]$	$[0]$	$[-\frac{1}{3}]$
$\bar{B}^0 \to \bar{K}^0K^0$	1	0	0	1	1	$-\frac{1}{3}$	$-\frac{1}{3}$
		$[0]$	$[0]$	$[0]$	$[1]$	$[0]$	$[-\frac{1}{3}]$
$B^- \to \pi^-\eta^{(\prime)}$	$\frac{1}{\sqrt{2}}$	0	$1(q)$	$1(q)$	0	$\frac{2}{3}(q)$	0
		$[0]$	$[1(q)]$	$[1(q)]$	$[0]$	$[\frac{2}{3}(q)]$	$[0]$
$\bar{B}^0 \to \pi^0\eta^{(\prime)}$	$-\frac{1}{2}$	$-1(q)$	0	$1(q)$	0	$-\frac{1}{3}(q)$	$-1(q)$
		$[-1(q)]$	$[0]$	$[1(q)]$	$[0]$	$[-\frac{1}{3}(q)]$	$[-1(q)]$
$\bar{B}^0 \to \eta^{(\prime)}\eta^{(\prime)}$	$\frac{1}{2}$	$1(q,q)$	0	$1(q,q)$	$2(q,q)+2(s,s)$	$-\frac{1}{3}(q,q)$	$\frac{1}{3}(q,q)-\frac{2}{3}(s,s)$
		$[1(q,q)]$	$[0]$	$[1(q,q)]$	$[2(q,q)+2(s,s)]$	$[-\frac{1}{3}(q,q)]$	$[\frac{1}{3}(q,q)-\frac{2}{3}(s,s)]$

TABLE III: (*Continued from Table II*) Singlet weak annihilation contributions.

$\bar{B} \to P_1 P_2$	factor	$SE^{(\zeta)}_{P_1\ [P_2]}$	$SA^{(\zeta)}_{P_1\ [P_2]}$	$SPE^{(\zeta)}_{P_1\ [P_2]}$	$SPA^{(\zeta)}_{P_1\ [P_2]}$	$SPE^{(\zeta)}_{\mathrm{EW},\ P_1\ [P_2]}$	$SPA^{(\zeta)}_{\mathrm{EW},\ P_1\ [P_2]}$
$B^- \to \pi^- \eta^{(\prime)}$	$\frac{1}{\sqrt{2}}$	0	$2(q)+\sqrt{2}(s)$	$2(q)+\sqrt{2}(s)$	0	$\frac{4}{3}(q)+\frac{2\sqrt{2}}{3}(s)$	0
		$[0]$	$[0]$	$[0]$	$[0]$	$[0]$	$[0]$
$\bar{B}^0 \to \pi^0 \eta^{(\prime)}$	$-\frac{1}{2}$	$-2(q)-\sqrt{2}(s)$	0	$2(q)+\sqrt{2}(s)$	0	$-\frac{2}{3}(q)-\frac{\sqrt{2}}{3}(s)$	$-2(q)-\sqrt{2}(s)$
		$[0]$	$[0]$	$[0]$	$[0]$	$[0]$	$[0]$
$\bar{B}^0 \to \eta^{(\prime)} \eta^{(\prime)}$	$\frac{1}{2}$	$2(q,q)$	0	$2(q,q)$	$4(q,q)+2\sqrt{2}(q,s)$	$-\frac{2}{3}(q,q)$	$\frac{2}{3}(q,q)+\frac{\sqrt{2}}{3}(q,s)$
		$+\sqrt{2}(q,s)$		$+\sqrt{2}(q,s)$	$+2\sqrt{2}(s,q)+2(s,s)$	$-\frac{\sqrt{2}}{3}(q,s)$	$-\frac{2\sqrt{2}}{3}(s,q)-\frac{2}{3}(s,s)$
		$[2(q,q)$	$[0]$	$[2(q,q)$	$[4(q,q)+2\sqrt{2}(q,s)$	$[-\frac{2}{3}(q,q)$	$[\frac{2}{3}(q,q)+\frac{\sqrt{2}}{3}(q,s)$
		$+\sqrt{2}(q,s)]$		$+\sqrt{2}(q,s)]$	$+2\sqrt{2}(s,q)+2(s,s)]$	$-\frac{\sqrt{2}}{3}(q,s)]$	$-\frac{2\sqrt{2}}{3}(s,q)-\frac{2}{3}(s,s)]$

TABLE IV: Coefficients of $\mathrm{SU(3)_F}$ amplitudes in $\bar{B} \to P_1 P_2$ ($|\Delta S| = 1$).

$\bar{B} \to P_1 P_2$	factor	$T'^{(\zeta)}_{P_1\ [P_2]}$	$C'^{(\zeta)}_{P_1\ [P_2]}$	$S'^{(\zeta)}_{P_1\ [P_2]}$	$P'^{(\zeta)}_{P_1\ [P_2]}$	$P'^{(\zeta)}_{\mathrm{EW},\ P_1\ [P_2]}$	$P^{C\prime,\ (\zeta)}_{\mathrm{EW},\ P_1\ [P_2]}$
$B^- \to \pi^- \bar{K}^0$	1	0	0	0	1	0	$-\frac{1}{3}$
		$[0]$	$[0]$	$[0]$	$[0]$	$[0]$	$[0]$
$B^- \to \pi^0 K^-$	$\frac{1}{\sqrt{2}}$	1	0	0	1	0	$\frac{2}{3}$
		$[0]$	$[1]$	$[0]$	$[0]$	$[1]$	$[0]$
$\bar{B}^0 \to \pi^+ K^-$	1	1	0	0	1	0	$\frac{2}{3}$
		$[0]$	$[0]$	$[0]$	$[0]$	$[0]$	$[0]$
$\bar{B}^0 \to \pi^0 \bar{K}^0$	$\frac{1}{\sqrt{2}}$	0	0	0	-1	0	$\frac{1}{3}$
		$[0]$	$[1]$	$[0]$	$[0]$	$[1]$	$[0]$
$B^- \to K^- \eta^{(\prime)}$	$\frac{1}{\sqrt{2}}$	0	$1(q)+\sqrt{2}(c)$	$2(q)+\sqrt{2}(s)+\sqrt{2}(c)$	$\sqrt{2}(s)$	$\frac{1}{3}(q)-\frac{\sqrt{2}}{3}(s)$	$-\frac{\sqrt{2}}{3}(s)$
		$[1(q)]$	$[0]$	$[0]$	$[1(q)]$	$[0]$	$[\frac{2}{3}(q)]$
$\bar{B}^0 \to \bar{K}^0 \eta^{(\prime)}$	$\frac{1}{\sqrt{2}}$	0	$1(q)+\sqrt{2}(c)$	$2(q)+\sqrt{2}(s)+\sqrt{2}(c)$	$\sqrt{2}(s)$	$\frac{1}{3}(q)-\frac{\sqrt{2}}{3}(s)$	$-\frac{\sqrt{2}}{3}(s)$
		$[0]$	$[0]$	$[0]$	$[1(q)]$	$[0]$	$[-\frac{1}{3}(q)]$

TABLE V: (*Continued from Table IV*) Weak annihilation contributions.

$\bar{B} \to P_1 P_2$	factor	$E'^{(\zeta)}_{P_1\ [P_2]}$	$A'^{(\zeta)}_{P_1\ [P_2]}$	$PE'^{(\zeta)}_{P_1\ [P_2]}$	$PA'^{(\zeta)}_{P_1\ [P_2]}$	$PE'^{(\zeta)}_{\mathrm{EW},\ P_1\ [P_2]}$	$PA'^{(\zeta)}_{\mathrm{EW},\ P_1\ [P_2]}$
$B^- \to \pi^- \bar{K}^0$	1	0	1	1	0	$\frac{2}{3}$	0
		[0]	[0]	[0]	[0]	[0]	[0]
$B^- \to \pi^0 K^-$	$\frac{1}{\sqrt{2}}$	0	1	1	0	$\frac{2}{3}$	0
		[0]	[0]	[0]	[0]	[0]	[0]
$\bar{B}^0 \to \pi^+ K^-$	1	0	0	1	0	$-\frac{1}{3}$	0
		[0]	[0]	[0]	[0]	[0]	[0]
$\bar{B}^0 \to \pi^0 \bar{K}^0$	$\frac{1}{\sqrt{2}}$	0	0	-1	0	$\frac{1}{3}$	0
		[0]	[0]	[0]	[0]	[0]	[0]
$B^- \to K^- \eta^{(\prime)}$	$\frac{1}{\sqrt{2}}$	0	$\sqrt{2}(s)$	$\sqrt{2}(s)$	0	$\frac{2\sqrt{2}}{3}(s)$	0
		[0]	$[1(q)]$	$[1(q)]$	[0]	$[\frac{2}{3}(q)]$	[0]
$\bar{B}^0 \to \bar{K}^0 \eta^{(\prime)}$	$\frac{1}{\sqrt{2}}$	0	0	$\sqrt{2}(s)$	0	$-\frac{\sqrt{2}}{3}(s)$	0
		[0]	[0]	$[1(q)]$	[0]	$[-\frac{1}{3}(q)]$	[0]

TABLE VI: (*Continued from Table V*) Singlet weak annihilation contributions.

$\bar{B} \to P_1 P_2$	factor	$SE'^{(\zeta)}_{P_1\ [P_2]}$	$SA'^{(\zeta)}_{P_1\ [P_2]}$	$SPE'^{(\zeta)}_{P_1\ [P_2]}$	$SPA'^{(\zeta)}_{P_1\ [P_2]}$	$SPE'^{(\zeta)}_{\mathrm{EW},\ P_1\ [P_2]}$	$SPA'^{(\zeta)}_{\mathrm{EW},\ P_1\ [P_2]}$
$B^- \to K^- \eta^{(\prime)}$	$\frac{1}{\sqrt{2}}$	0	$2(q) + \sqrt{2}(s)$	$2(q) + \sqrt{2}(s)$	0	$\frac{4}{3}(q) + \frac{2\sqrt{2}}{3}(s)$	0
		[0]	[0]	[0]	[0]	[0]	[0]
$\bar{B}^0 \to \bar{K}^0 \eta^{(\prime)}$	$\frac{1}{\sqrt{2}}$	0	0	$2(q) + \sqrt{2}(s)$	0	$-\frac{2}{3}(q) - \frac{\sqrt{2}}{3}(s)$	0
		[0]	[0]	[0]	[0]	[0]	[0]

TABLE VII: Coefficients of $\mathrm{SU(3)_F}$ amplitudes in $\bar{B} \to PV$ ($\Delta S = 0$). When ideal mixing for ω and ϕ is assumed, i) for $B^- \to \pi^-\omega$ ($\pi^-\phi$) and $\bar{B}^0 \to \pi^0\omega$ ($\pi^0\phi$), set the coefficients of $\mathrm{SU(3)_F}$ amplitudes with the subscript π and the superscript $\zeta = s$ (q) to zero: *i.e.*, for $\bar{B} \to \pi\omega$, $S_\pi^{(s)} = P_{\mathrm{EW},\pi}^{(s)} = 0$, and for $\bar{B} \to \pi\phi$, $C_\pi^{(q)} = S_\pi^{(q)} = P_\pi^{(q)} = \cdots = 0$, and ii) for $\bar{B}^0 \to \eta^{(\prime)}\omega$ [$\eta^{(\prime)}\phi$], set the coefficients of $\mathrm{SU(3)_F}$ amplitudes with the subscript $\eta^{(\prime)}$ and the superscript $\zeta = (q,s)$ or (s,s) [(q,q) or (s,q)] to zero: *i.e.*, for $\bar{B}^0 \to \eta^{(\prime)}\omega$, $S_{\eta^{(\prime)}}^{(q,s)} = P_{\mathrm{EW},\eta^{(\prime)}}^{(q,s)} = 0$, and for $\bar{B}^0 \to \eta^{(\prime)}\phi$, $C_{\eta^{(\prime)}}^{(q,q)} = S_{\eta^{(\prime)}}^{(q,q)} = P_{\eta^{(\prime)}}^{(q,q)} = \cdots = 0$.

$\bar{B} \to PV$	factor	$T_{P\ [V]}^{(\zeta)}$	$C_{P\ [V]}^{(\zeta)}$	$S_{P\ [V]}^{(\zeta)}$	$P_{P\ [V]}^{(\zeta)}$	$P_{\mathrm{EW},\ P\ [V]}^{(\zeta)}$	$P_{\mathrm{EW},\ P\ [V]}^{C,\ (\zeta)}$
$B^- \to \pi^-\rho^0$	$\frac{1}{\sqrt{2}}$	0	1	0	-1	1	$\frac{1}{3}$
		[1]	[0]	[0]	[1]	[0]	$[\frac{2}{3}]$
$B^- \to \pi^0\rho^-$	$\frac{1}{\sqrt{2}}$	1	0	0	1	0	$\frac{2}{3}$
		[0]	[1]	[0]	$[-1]$	[1]	$[\frac{1}{3}]$
$\bar{B}^0 \to \pi^+\rho^-$	1	1	0	0	1	0	$\frac{2}{3}$
		[0]	[0]	[0]	[0]	[0]	[0]
$\bar{B}^0 \to \pi^-\rho^+$	1	0	0	0	0	0	0
		[1]	[0]	[0]	[1]	[0]	$[\frac{2}{3}]$
$\bar{B}^0 \to \pi^0\rho^0$	$-\frac{1}{2}$	0	1	0	-1	1	$\frac{1}{3}$
		[0]	[1]	[0]	$[-1]$	[1]	$[\frac{1}{3}]$
$B^- \to K^-K^{*0}$	1	0	0	0	1	0	$-\frac{1}{3}$
		[0]	[0]	[0]	[0]	[0]	[0]
$B^- \to K^0K^{*-}$	1	0	0	0	0	0	0
		[0]	[0]	[0]	[1]	[0]	$[-\frac{1}{3}]$
$\bar{B}^0 \to K^-K^{*+}$	1	0	0	0	0	0	0
		[0]	[0]	[0]	[0]	[0]	[0]
$\bar{B}^0 \to K^+K^{*-}$	1	0	0	0	0	0	0
		[0]	[0]	[0]	[0]	[0]	[0]
$\bar{B}^0 \to \bar{K}^0K^{*0}$	1	0	0	0	1	0	$-\frac{1}{3}$
		[0]	[0]	[0]	[0]	[0]	[0]
$\bar{B}^0 \to K^0\bar{K}^{*0}$	1	0	0	0	0	0	0
		[0]	[0]	[0]	[1]	[0]	$[-\frac{1}{3}]$
$B^- \to \eta^{(\prime)}\rho^-$	$\frac{1}{\sqrt{2}}$	$1(q)$	0	0	$1(q)$	0	$\frac{2}{3}(q)$
		[0]	$[1(q) + \sqrt{2}(c)]$	$[2(q) + \sqrt{2}(s) + \sqrt{2}(c)]$	$[1(q)]$	$[\frac{1}{3}(q) - \frac{\sqrt{2}}{3}(s)]$	$[-\frac{1}{3}(q)]$
$\bar{B}^0 \to \eta^{(\prime)}\rho^0$	$-\frac{1}{2}$	0	$-1(q)$	0	$1(q)$	$-1(q)$	$-\frac{1}{3}(q)$
		[0]	$[1(q) + \sqrt{2}(c)]$	$[2(q) + \sqrt{2}(s) + \sqrt{2}(c)]$	$[1(q)]$	$[\frac{1}{3}(q) - \frac{\sqrt{2}}{3}(s)]$	$[-\frac{1}{3}(q)]$
$B^- \to \pi^-\ \omega/\phi$	$\frac{1}{\sqrt{2}}$	0	$1(q)$	$2(q) + \sqrt{2}(s)$	$1(q)$	$\frac{1}{3}(q) - \frac{\sqrt{2}}{3}(s)$	$-\frac{1}{3}(q)$
		$[1(q)]$	[0]	[0]	$[1(q)]$	[0]	$[\frac{2}{3}(q)]$
$\bar{B}^0 \to \pi^0\ \omega/\phi$	$-\frac{1}{2}$	0	$1(q)$	$2(q) + \sqrt{2}(s)$	$1(q)$	$\frac{1}{3}(q) - \frac{\sqrt{2}}{3}(s)$	$-\frac{1}{3}(q)$
		[0]	$[-1(q)]$	[0]	$[1(q)]$	$[-1(q)]$	$[-\frac{1}{3}(q)]$
$\bar{B}^0 \to \eta^{(\prime)}\ \omega/\phi$	$\frac{1}{2}$	0	$1(q,q)$	$2(q,q) + \sqrt{2}(q,s)$	$1(q,q)$	$\frac{1}{3}(q,q) - \frac{\sqrt{2}}{3}(q,s)$	$-\frac{1}{3}(q,q)$
		[0]	$[1(q,q) + \sqrt{2}(q,c)]]$	$[2(q,q) + \sqrt{2}(q,s)$ $+\sqrt{2}(q,c)]]$	$[1(q,q)$	$[\frac{1}{3}(q,q) - \frac{\sqrt{2}}{3}(q,s)]$	$[-\frac{1}{3}(q,q)]$

TABLE VIII: (*Continued from Table VII*) Weak annihilation contributions. When ideal mixing for ω and ϕ is assumed, the same rules as used in *Table VII* are applied.

$\bar{B} \to PV$	factor	$E_{P\ [V]}^{(\zeta)}$	$A_{P\ [V]}^{(\zeta)}$	$PE_{P\ [V]}^{(\zeta)}$	$PA_{P\ [V]}^{(\zeta)}$	$PE_{\mathrm{EW},\ P\ [V]}^{(\zeta)}$	$PA_{\mathrm{EW},\ P\ [V]}^{(\zeta)}$
$B^- \to \pi^- \rho^0$	$\frac{1}{\sqrt{2}}$	0	-1	-1	0	$-\frac{2}{3}$	0
		$[0]$	$[1]$	$[1]$	$[0]$	$[\frac{2}{3}]$	$[0]$
$B^- \to \pi^0 \rho^-$	$\frac{1}{\sqrt{2}}$	0	1	1	0	$\frac{2}{3}$	0
		$[0]$	$[-1]$	$[-1]$	$[0]$	$[-\frac{2}{3}]$	$[0]$
$\bar{B}^0 \to \pi^+ \rho^-$	1	0	0	1	1	$-\frac{1}{3}$	$-\frac{1}{3}$
		$[1]$	$[0]$	$[0]$	$[1]$	$[0]$	$[\frac{2}{3}]$
$\bar{B}^0 \to \pi^- \rho^+$	1	1	0	0	1	0	$\frac{2}{3}$
		$[0]$	$[0]$	$[1]$	$[1]$	$[-\frac{1}{3}]$	$[-\frac{1}{3}]$
$\bar{B}^0 \to \pi^0 \rho^0$	$-\frac{1}{2}$	-1	0	-1	-2	$\frac{1}{3}$	$-\frac{1}{3}$
		$[-1]$	$[0]$	$[-1]$	$[-2]$	$[\frac{1}{3}]$	$[-\frac{1}{3}]$
$B^- \to K^- K^{*0}$	1	0	1	1	0	$\frac{2}{3}$	0
		$[0]$	$[0]$	$[0]$	$[0]$	$[0]$	$[0]$
$B^- \to K^0 K^{*-}$	1	0	0	0	0	0	0
		$[0]$	$[1]$	$[1]$	$[0]$	$[\frac{2}{3}]$	$[0]$
$\bar{B}^0 \to K^- K^{*+}$	1	1	0	0	1	0	$\frac{2}{3}$
		$[0]$	$[0]$	$[0]$	$[1]$	$[0]$	$[-\frac{1}{3}]$
$\bar{B}^0 \to K^+ K^{*-}$	1	0	0	0	1	0	$-\frac{1}{3}$
		$[1]$	$[0]$	$[0]$	$[1]$	$[0]$	$[\frac{2}{3}]$
$\bar{B}^0 \to \bar{K}^0 K^{*0}$	1	0	0	1	1	$-\frac{1}{3}$	$-\frac{1}{3}$
		$[0]$	$[0]$	$[0]$	$[1]$	$[0]$	$[-\frac{1}{3}]$
$\bar{B}^0 \to K^0 \bar{K}^{*0}$	1	0	0	0	1	0	$-\frac{1}{3}$
		$[0]$	$[0]$	$[1]$	$[1]$	$[-\frac{1}{3}]$	$[-\frac{1}{3}]$
$B^- \to \eta^{(\prime)} \rho^-$	$\frac{1}{\sqrt{2}}$	0	$1(q)$	$1(q)$	0	$\frac{2}{3}(q)$	0
		$[0]$	$[1(q)]$	$[1(q)]$	$[0]$	$[\frac{2}{3}(q)]$	$[0]$
$\bar{B}^0 \to \eta^{(\prime)} \rho^0$	$-\frac{1}{2}$	$-1(q)$	0	$1(q)$	0	$-\frac{1}{3}(q)$	$-1(q)$
		$[-1(q)]$	$[0]$	$[1(q)]$	$[0]$	$[-\frac{1}{3}(q)]$	$[-1(q)]$
$B^- \to \pi^-\ \omega/\phi$	$\frac{1}{\sqrt{2}}$	0	$1(q)$	$1(q)$	0	$\frac{2}{3}(q)$	0
		$[0]$	$[1(q)]$	$[1(q)]$	$[0]$	$[\frac{2}{3}(q)]$	$[0]$
$\bar{B}^0 \to \pi^0\ \omega/\phi$	$-\frac{1}{2}$	$-1(q)$	0	$1(q)$	0	$-\frac{1}{3}(q)$	$-1(q)$
		$[-1(q)]$	$[0]$	$[1(q)]$	$[0]$	$[-\frac{1}{3}(q)]$	$[-1(q)]$
$\bar{B}^0 \to \eta^{(\prime)}\ \omega/\phi$	$\frac{1}{2}$	$1(q,q)$	0	$1(q,q)$	$2(q,q)+2(s,s)$	$-\frac{1}{3}(q,q)$	$\frac{1}{3}(q,q)-\frac{2}{3}(s,s)$
		$[1(q,q)]$	$[0]$	$[1(q,q)]$	$[2(q,q)+2(s,s)]$	$[-\frac{1}{3}(q,q)]$	$[\frac{1}{3}(q,q)-\frac{2}{3}(s,s)]$

TABLE IX: (*Continued from Table VIII*) Singlet weak annihilation contributions. When ideal mixing for ω and ϕ is assumed, the same rules as used in *Table VII* are applied.

$\bar{B} \to PV$	factor	$SE^{(\zeta)}_{P\ [V]}$	$SA^{(\zeta)}_{P\ [V]}$	$SPE^{(\zeta)}_{P\ [V]}$	$SPA^{(\zeta)}_{P\ [V]}$	$SPE^{(\zeta)}_{\mathrm{EW},\ P\ [V]}$	$SPA^{(\zeta)}_{\mathrm{EW},\ P\ [V]}$
$B^- \to \eta^{(\prime)}\rho^-$	$\frac{1}{\sqrt{2}}$	0	0	0	0	0	0
		$[0]$	$[2(q)+\sqrt{2}(s)]$	$[2(q)+\sqrt{2}(s)]$	$[0]$	$[\frac{4}{3}(q)+\frac{2\sqrt{2}}{3}(s)]$	$[0]$
$\bar{B}^0 \to \eta^{(\prime)}\rho^0$	$-\frac{1}{2}$	0	0	0	0	0	0
		$[-2(q)-\sqrt{2}(s)]$	$[0]$	$[2(q)+\sqrt{2}(s)]$	$[0]$	$[-\frac{2}{3}(q)-\frac{\sqrt{2}}{3}(s)]$	$[-2(q)-\sqrt{2}(s)]$
$B^- \to \pi^-\ \omega/\phi$	$\frac{1}{\sqrt{2}}$	0	$2(q)+\sqrt{2}(s)$	$2(q)+\sqrt{2}(s)$	0	$\frac{4}{3}(q)+\frac{2\sqrt{2}}{3}(s)$	0
		$[0]$	$[0]$	$[0]$	$[0]$	$[0]$	$[0]$
$\bar{B}^0 \to \pi^0\ \omega/\phi$	$-\frac{1}{2}$	$-2(q)-\sqrt{2}(s)$	0	$2(q)+\sqrt{2}(s)$	0	$-\frac{2}{3}(q)-\frac{\sqrt{2}}{3}(s)$	$-2(q)-\sqrt{2}(s)$
		$[0]$	$[0]$	$[0]$	$[0]$	$[0]$	$[0]$
$\bar{B}^0 \to \eta^{(\prime)}\ \omega/\phi$	$\frac{1}{2}$	$2(q,q)$	0	$2(q,q)$	$4(q,q)+2\sqrt{2}(q,s)$	$-\frac{2}{3}(q,q)$	$\frac{2}{3}(q,q)+\frac{\sqrt{2}}{3}(q,s)$
		$+\sqrt{2}(q,s)$		$+\sqrt{2}(q,s)$	$+2\sqrt{2}(s,q)+2(s,s)$	$-\frac{\sqrt{2}}{3}(q,s)$	$-\frac{2\sqrt{2}}{3}(s,q)-\frac{2}{3}(s,s)$
		$[2(q,q)$	$[0]$	$[2(q,q)$	$[4(q,q)+2\sqrt{2}(q,s)$	$[-\frac{2}{3}(q,q)$	$[\frac{2}{3}(q,q)+\frac{\sqrt{2}}{3}(q,s)$
		$+\sqrt{2}(q,s)]$		$+\sqrt{2}(q,s)]$	$+2\sqrt{2}(s,q)+2(s,s)]$	$-\frac{\sqrt{2}}{3}(q,s)]$	$-\frac{2\sqrt{2}}{3}(s,q)-\frac{2}{3}(s,s)]$

TABLE X: Coefficients of $\mathrm{SU(3)_F}$ amplitudes in $\bar{B} \to PV$ ($|\Delta S| = 1$). When ideal mixing for ω and ϕ is assumed, for $B^- \to K^-\omega$ ($K^-\phi$) and $\bar{B}^0 \to K^0\omega$ ($K^0\phi$), set the coefficients of $\mathrm{SU(3)_F}$ amplitudes with the subscript K and the superscript $\zeta = s$ (q) to zero: *i.e.*, for $\bar{B} \to K\omega$, $S_K^{\prime(s)} = P_K^{\prime(s)} = \cdots = 0$, and for $\bar{B} \to K\phi$, $C_K^{\prime(q)} = S_K^{\prime(q)} = P_{\mathrm{EW},K}^{\prime(q)} = 0$.

$\bar{B} \to PV$	factor	$T_{P\ [V]}^{\prime(\zeta)}$	$C_{P\ [V]}^{\prime(\zeta)}$	$S_{P\ [V]}^{\prime(\zeta)}$	$P_{P\ [V]}^{\prime(\zeta)}$	$P_{\mathrm{EW},\ P\ [V]}^{\prime(\zeta)}$	$P_{\mathrm{EW},\ P\ [V]}^{C\prime,\ (\zeta)}$
$B^- \to \pi^- \bar{K}^{*0}$	1	0	0	0	1	0	$-\frac{1}{3}$
		[0]	[0]	[0]	[0]	[0]	[0]
$B^- \to \pi^0 K^{*-}$	$\frac{1}{\sqrt{2}}$	1	0	0	1	0	$\frac{2}{3}$
		[0]	[1]	[0]	[0]	[1]	[0]
$\bar{B}^0 \to \pi^+ K^{*-}$	1	1	0	0	1	0	$\frac{2}{3}$
		[0]	[0]	[0]	[0]	[0]	[0]
$\bar{B}^0 \to \pi^0 \bar{K}^{*0}$	$\frac{1}{\sqrt{2}}$	0	0	0	-1	0	$\frac{1}{3}$
		[0]	[1]	[0]	[0]	[1]	[0]
$B^- \to \bar{K}^0 \rho^-$	1	0	0	0	0	0	
		[0]	[0]	[0]	[1]	[0]	$[-\frac{1}{3}]$
$B^- \to K^- \rho^0$	$\frac{1}{\sqrt{2}}$	0	1	0	0	1	0
		[1]	[0]	[0]	[1]	[0]	$[\frac{2}{3}]$
$\bar{B}^0 \to K^- \rho^+$	1	0	0	0	0	0	0
		[1]	[0]	[0]	[1]	[0]	$[\frac{2}{3}]$
$\bar{B}^0 \to \bar{K}^0 \rho^0$	$\frac{1}{\sqrt{2}}$	0	1	0	0	1	0
		[0]	[0]	[0]	$[-1]$	[0]	$[\frac{1}{3}]$
$B^- \to \eta^{(\prime)} K^{*-}$	$\frac{1}{\sqrt{2}}$	$1(q)$	0	0	$1(q)$	0	$\frac{2}{3}(q)$
		[0]	$[1(q) + \sqrt{2}(c)]$	$[2(q) + \sqrt{2}(s) + \sqrt{2}(c)]$	$[\sqrt{2}(s)]$	$[\frac{1}{3}(q) - \frac{\sqrt{2}}{3}(s)]$	$[-\frac{\sqrt{2}}{3}(s)]$
$\bar{B}^0 \to \eta^{(\prime)} \bar{K}^{*0}$	$\frac{1}{\sqrt{2}}$	0	0	0	$1(q)$	0	$-\frac{1}{3}(q)$
		[0]	$[1(q) + \sqrt{2}(c)]$	$[2(q) + \sqrt{2}(s) + \sqrt{2}(c)]$	$[\sqrt{2}(s)]$	$[\frac{1}{3}(q) - \frac{\sqrt{2}}{3}(s)]$	$[-\frac{\sqrt{2}}{3}(s)]$
$B^- \to K^-\ \omega/\phi$	$\frac{1}{\sqrt{2}}$	0	$1(q)$	$2(q) + \sqrt{2}(s)$	$\sqrt{2}(s)$	$\frac{1}{3}(q) - \frac{\sqrt{2}}{3}(s)$	$-\frac{\sqrt{2}}{3}(s)$
		$[1(q)]$	[0]	[0]	$[1(q)]$	[0]	$[\frac{2}{3}(q)]$
$\bar{B}^0 \to \bar{K}^0\ \omega/\phi$	$\frac{1}{\sqrt{2}}$	0	$1(q)$	$2(q) + \sqrt{2}(s)$	$\sqrt{2}(s)$	$\frac{1}{3}(q) - \frac{\sqrt{2}}{3}(s)$	$-\frac{\sqrt{2}}{3}(s)$
		[0]	[0]	[0]	$[1(q)]$	[0]	$[-\frac{1}{3}(q)]$

TABLE XI: (*Continued from Table X*) Weak annihilation contributions. When ideal mixing for ω and ϕ is assumed, the same rules as used in *Table X* are applied.

$\bar{B} \to PV$	factor	$E'^{(\zeta)}_{P\ [V]}$	$A'^{(\zeta)}_{P\ [V]}$	$PE'^{(\zeta)}_{P\ [V]}$	$PA'^{(\zeta)}_{P\ [V]}$	$PE'^{(\zeta)}_{\mathrm{EW},\ P\ [V]}$	$PA'^{(\zeta)}_{\mathrm{EW},\ P\ [V]}$
$B^- \to \pi^- \bar{K}^{*0}$	1	0	1	1	0	$\frac{2}{3}$	0
		[0]	[0]	[0]	[0]	[0]	[0]
$B^- \to \pi^0 K^{*-}$	$\frac{1}{\sqrt{2}}$	0	1	1	0	$\frac{2}{3}$	0
		[0]	[0]	[0]	[0]	[0]	[0]
$\bar{B}^0 \to \pi^+ K^{*-}$	1	0	0	1	0	$-\frac{1}{3}$	0
		[0]	[0]	[0]	[0]	[0]	[0]
$\bar{B}^0 \to \pi^0 \bar{K}^{*0}$	$\frac{1}{\sqrt{2}}$	0	0	-1	0	$\frac{1}{3}$	0
		[0]	[0]	[0]	[0]	[0]	[0]
$B^- \to \bar{K}^0 \rho^-$	1	0	0	0	0	0	0
		[0]	[1]	[1]	[0]	$[\frac{2}{3}]$	[0]
$B^- \to K^- \rho^0$	$\frac{1}{\sqrt{2}}$	0	0	0	0	0	0
		[0]	[1]	[1]	[0]	$[\frac{2}{3}]$	[0]
$\bar{B}^0 \to K^- \rho^+$	1	0	0	0	0	0	0
		[0]	[0]	[1]	[0]	$[-\frac{1}{3}]$	[0]
$\bar{B}^0 \to \bar{K}^{*0} \rho^0$	$\frac{1}{\sqrt{2}}$	0	0	0	0	0	0
		[0]	[0]	$[-1]$	[0]	$[\frac{1}{3}]$	[0]
$B^- \to \eta^{(\prime)} K^{*-}$	$\frac{1}{\sqrt{2}}$	0	$1(q)$	$1(q)$	0	$\frac{2}{3}(q)$	0
		[0]	$[\sqrt{2}(s)]$	$[\sqrt{2}(s)]$	[0]	$[\frac{2\sqrt{2}}{3}(s)]$	[0]
$\bar{B}^0 \to \eta^{(\prime)} \bar{K}^{*0}$	$\frac{1}{\sqrt{2}}$	0	0	$1(q)$	0	$-\frac{1}{3}(q)$	0
		[0]	[0]	$[\sqrt{2}(s)]$	[0]	$[-\frac{\sqrt{2}}{3}(s)]$	[0]
$B^- \to K^-\ \omega/\phi$	$\frac{1}{\sqrt{2}}$	0	$\sqrt{2}(s)$	$\sqrt{2}(s)$	0	$\frac{2\sqrt{2}}{3}(s)$	0
		[0]	$[1(q)]$	$[1(q)]$	[0]	$[\frac{2}{3}(q)]$	[0]
$\bar{B}^0 \to \bar{K}^0\ \omega/\phi$	$\frac{1}{\sqrt{2}}$	0	0	$\sqrt{2}(s)$	0	$-\frac{\sqrt{2}}{3}(s)$	0
		[0]	[0]	$[1(q)]$	[0]	$[-\frac{1}{3}(q)]$	[0]

TABLE XII: (*Continued from Table XI*) Singlet weak annihilation contributions. When ideal mixing for ω and ϕ is assumed, the same rules as used in *Table X* are applied.

$\bar{B} \to PV$	factor	$SE'^{(\zeta)}_{P\ [V]}$	$SA'^{(\zeta)}_{P\ [V]}$	$SPE'^{(\zeta)}_{P\ [V]}$	$SPA'^{(\zeta)}_{P\ [V]}$	$SPE'^{(\zeta)}_{\mathrm{EW},\ P\ [V]}$	$SPA'^{(\zeta)}_{\mathrm{EW},\ P\ [V]}$
$B^- \to \eta^{(\prime)} K^{*-}$	$\frac{1}{\sqrt{2}}$	0	0	0	0	0	0
		[0]	$[2(q)+\sqrt{2}(s)]$	$[2(q)+\sqrt{2}(s)]$	[0]	$[\frac{4}{3}(q)+\frac{2\sqrt{2}}{3}(s)]$	[0]
$\bar{B}^0 \to \eta^{(\prime)} \bar{K}^{*0}$	$\frac{1}{\sqrt{2}}$	0	0	0	0	0	0
		[0]	[0]	$[2(q)+\sqrt{2}(s)]$	[0]	$[-\frac{2}{3}(q)-\frac{\sqrt{2}}{3}(s)]$	[0]
$B^- \to K^- \ \omega/\phi$	$\frac{1}{\sqrt{2}}$	0	$2(q)+\sqrt{2}(s)$	$2(q)+\sqrt{2}(s)$	0	$\frac{4}{3}(q)+\frac{2\sqrt{2}}{3}(s)$	0
		[0]	[0]	[0]	[0]	[0]	[0]
$\bar{B}^0 \to \bar{K}^0 \ \omega/\phi$	$\frac{1}{\sqrt{2}}$	0	0	$2(q)+\sqrt{2}(s)$	0	$-\frac{2}{3}(q)-\frac{\sqrt{2}}{3}(s)$	0
		[0]	[0]	[0]	[0]	[0]	[0]

TABLE XIII: Coefficients of $\mathrm{SU(3)_F}$ amplitudes in $\bar{B}_s \to P_1 P_2$ ($\Delta S = 0$).

$\bar{B}_s \to P_1 P_2$	factor	$T^{(\zeta)}_{P_1\ [P_2]}$	$C^{(\zeta)}_{P_1\ [P_2]}$	$S^{(\zeta)}_{P_1\ [P_2]}$	$P^{(\zeta)}_{P_1\ [P_2]}$	$P^{(\zeta)}_{\mathrm{EW},\ P_1\ [P_2]}$	$P^{C,\ (\zeta)}_{\mathrm{EW},\ P_1\ [P_2]}$
$\bar{B}_s \to K^+\pi^-$	1	1	0	0	1	0	$\frac{2}{3}$
		[0]	[0]	[0]	[0]	[0]	[0]
$\bar{B}_s \to K^0\pi^0$	$\frac{1}{\sqrt{2}}$	0	1	0	-1	1	$\frac{1}{3}$
		[0]	[0]	[0]	[0]	[0]	[0]
$\bar{B}_s \to K^0\eta^{(\prime)}$	$\frac{1}{\sqrt{2}}$	0	$1(q)+\sqrt{2}(c)$	$2(q)+\sqrt{2}(s)+\sqrt{2}(c)$	$1(q)$	$\frac{1}{3}(q)-\frac{\sqrt{2}}{3}(s)$	$-\frac{1}{3}(q)$
		[0]	[0]	[0]	$[\sqrt{2}(s)]$	[0]	$[-\frac{\sqrt{2}}{3}(s)]$

TABLE XIV: (*Continued from Table XIII*) Weak annihilation contributions.

$\bar{B}_s \to P_1P_2$	factor	$E^{(\zeta)}_{P_1\ [P_2]}$	$A^{(\zeta)}_{P_1\ [P_2]}$	$PE^{(\zeta)}_{P_1\ [P_2]}$	$PA^{(\zeta)}_{P_1\ [P_2]}$	$PE^{(\zeta)}_{\mathrm{EW},\ P_1\ [P_2]}$	$PA^{(\zeta)}_{\mathrm{EW},\ P_1\ [P_2]}$
$\bar{B}_s \to K^+\pi^-$	1	0	0	1	0	$-\frac{1}{3}$	0
		[0]	[0]	[0]	[0]	[0]	[0]
$\bar{B}_s \to K^0\pi^0$	$\frac{1}{\sqrt{2}}$	0	0	-1	0	$\frac{1}{3}$	0
		[0]	[0]	[0]	[0]	[0]	[0]
$\bar{B}_s \to K^0\eta^{(\prime)}$	$\frac{1}{\sqrt{2}}$	0	0	$1(q)$	0	$-\frac{1}{3}(q)$	0
		[0]	[0]	$[\sqrt{2}(s)]$	[0]	$[-\frac{\sqrt{2}}{3}(s)]$	[0]

TABLE XV: (*Continued from Table XIV*) Singlet weak annihilation contributions.

$\bar{B}_s \to P_1P_2$	factor	$SE^{(\zeta)}_{P_1\ [P_2]}$	$SA^{(\zeta)}_{P_1\ [P_2]}$	$SPE^{(\zeta)}_{P_1\ [P_2]}$	$SPA^{(\zeta)}_{P_1\ [P_2]}$	$SPE^{(\zeta)}_{\mathrm{EW},\ P_1\ [P_2]}$	$SPA^{(\zeta)}_{\mathrm{EW},\ P_1\ [P_2]}$
$\bar{B}_s \to K^0\eta^{(\prime)}$	$\frac{1}{\sqrt{2}}$	0	0	$2(q)+\sqrt{2}(s)$	0	$-\frac{2}{3}(q)-\frac{\sqrt{2}}{3}(s)$	0
		[0]	[0]	[0]	[0]	[0]	[0]

TABLE XVI: Coefficients of $\mathrm{SU(3)_F}$ amplitudes in $\bar{B}_s \to P_1P_2$ ($|\Delta S| = 1$).

$\bar{B}_s \to P_1P_2$	factor	$T'^{(\zeta)}_{P_1\ [P_2]}$	$C'^{(\zeta)}_{P_1\ [P_2]}$	$S'^{(\zeta)}_{P_1\ [P_2]}$	$P'^{(\zeta)}_{P_1\ [P_2]}$	$P'^{(\zeta)}_{\mathrm{EW},\ P_1\ [P_2]}$	$P^{C\prime,\ (\zeta)}_{\mathrm{EW},\ P_1\ [P_2]}$
$\bar{B}_s \to \pi^+\pi^-$	1	0	0	0	0	0	0
		[0]	[0]	[0]	[0]	[0]	[0]
$\bar{B}_s \to \pi^0\pi^0$	$\frac{1}{2}$	0	0	0	0	0	0
		[0]	[0]	[0]	[0]	[0]	[0]
$\bar{B}_s \to \bar{K}^0K^0$	1	0	0	0	0	0	0
		[0]	[0]	[0]	[1]	[0]	$[-\frac{1}{3}]$
$\bar{B}_s \to K^-K^+$	1	0	0	0	0	0	0
		[1]	[0]	[0]	[1]	[0]	$[\frac{2}{3}]$
$\bar{B}_s \to \pi^0\eta^{(\prime)}$	$\frac{1}{2}$	0	0	0	0	0	0
		[0]	$[\sqrt{2}(s)]$	[0]	[0]	$[\sqrt{2}(s)]$	[0]
$\bar{B}_s \to \eta^{(\prime)}\eta^{(\prime)}$	$\frac{1}{2}$	0	$\sqrt{2}(s,q)$	$2\sqrt{2}(s,q)+2(s,s)$	$2(s,s)$	$\frac{\sqrt{2}}{3}(s,q)$	$-\frac{2}{3}(s,s)$
			$+2(s,c)$	$+2(s,c)$		$-\frac{2}{3}(s,s)$	
		[0]	$[\sqrt{2}(s,q)$	$[2\sqrt{2}(s,q)+2(s,s)$	$[2(s,s)]$	$[\frac{\sqrt{2}}{3}(s,q)$	$[-\frac{2}{3}(s,s)]$
			$+2(s,c)]$	$+2(s,c)]$		$-\frac{2}{3}(s,s)]$	

TABLE XVII: (*Continued from Table XVI*) Weak annihilation contributions.

$\bar{B}_s \to P_1 P_2$	factor	$E'^{(\zeta)}_{P_1\ [P_2]}$	$A'^{(\zeta)}_{P_1\ [P_2]}$	$PE'^{(\zeta)}_{P_1\ [P_2]}$	$PA'^{(\zeta)}_{P_1\ [P_2]}$	$PE'^{(\zeta)}_{\mathrm{EW},\ P_1\ [P_2]}$	$PA'^{(\zeta)}_{\mathrm{EW},\ P_1\ [P_2]}$
$\bar{B}_s \to \pi^+\pi^-$	1	0	0	0	1	0	$-\frac{1}{3}$
		[1]	[0]	[0]	[1]	[0]	$[\frac{2}{3}]$
$\bar{B}_s \to \pi^0\pi^0$	$\frac{1}{2}$	1	0	0	2	0	$\frac{1}{3}$
		[1]	[0]	[0]	[2]	[0]	$[\frac{1}{3}]$
$\bar{B}_s \to \bar{K}^0 K^0$	1	0	0	0	1	0	$-\frac{1}{3}$
		[0]	[0]	[1]	[1]	$[-\frac{1}{3}]$	$[-\frac{1}{3}]$
$\bar{B}_s \to K^- K^+$	1	1	0	0	1	0	$\frac{2}{3}$
		[0]	[0]	[1]	[1]	$[-\frac{1}{3}]$	$[-\frac{1}{3}]$
$\bar{B}_s \to \pi^0\eta^{(\prime)}$	$\frac{1}{2}$	$1(q)$	0	0	0	0	$1(q)$
		$[1(q)]$	[0]	[0]	[0]	[0]	$[1(q)]$
$\bar{B}_s \to \eta^{(\prime)}\eta^{(\prime)}$	$\frac{1}{2}$	$1(q,q)$	0	$2(s,s)$	$2(q,q)$	$-\frac{2}{3}(s,s)$	$\frac{1}{3}(q,q)$
					$+2(s,s)$		$-\frac{2}{3}(s,s)$
		$[1(q,q)]$	0	$[2(s,s)]$	$[2(q,q)$	$[-\frac{2}{3}(s,s)]$	$[\frac{1}{3}(q,q)$
					$+2(s,s)]$		$-\frac{2}{3}(s,s)]$

TABLE XVIII: (*Continued from Table XVII*) Singlet weak annihilation contributions.

$\bar{B}_s \to P_1 P_2$	factor	$SE'^{(\zeta)}_{P_1\ [P_2]}$	$SA'^{(\zeta)}_{P_1\ [P_2]}$	$SPE'^{(\zeta)}_{P_1\ [P_2]}$	$SPA'^{(\zeta)}_{P_1\ [P_2]}$	$SPE'^{(\zeta)}_{\mathrm{EW},\ P_1\ [P_2]}$	$SPA'^{(\zeta)}_{\mathrm{EW},\ P_1\ [P_2]}$
$\bar{B}_s \to \pi^0\eta^{(\prime)}$	$\frac{1}{2}$	$2(q)+\sqrt{2}(s)$	0	0	0	0	$2(q)+\sqrt{2}(s)$
		[0]	[0]	[0]	[0]	[0]	[0]
$\bar{B}_s \to \eta^{(\prime)}\eta^{(\prime)}$	$\frac{1}{2}$	$2(q,q)$	0	$2\sqrt{2}(s,q)$	$4(q,q)+2\sqrt{2}(q,s)$	$-\sqrt{2}(s,q)$	$\frac{2}{3}(q,q)+\frac{\sqrt{2}}{3}(q,s)$
		$+\sqrt{2}(q,s)$		$+2(s,s)$	$+2\sqrt{2}(s,q)+2(s,s)$	$-\frac{2}{3}(s,s)$	$-\sqrt{2}(s,q)-\frac{2}{3}(s,s)$
		$[2(q,q)$	[0]	$[2\sqrt{2}(s,q)$	$[4(q,q)+2\sqrt{2}(q,s)$	$[-\sqrt{2}(s,q)$	$[\frac{2}{3}(q,q)+\frac{\sqrt{2}}{3}(q,s)$
		$+\sqrt{2}(q,s)]$		$+2(s,s)]$	$+2\sqrt{2}(s,q)+2(s,s)]$	$-\frac{2}{3}(s,s)]$	$-\sqrt{2}(s,q)-\frac{2}{3}(s,s)]$

TABLE XIX: Coefficients of $\mathrm{SU(3)_F}$ amplitudes in $\bar{B}_s \to PV$ ($\Delta S = 0$). When ideal mixing for ω and ϕ is assumed, for $\bar{B}_s \to K^0\omega$ ($K^0\phi$), set the coefficients of $\mathrm{SU(3)_F}$ amplitudes with the subscript K and the superscript $\zeta = s$ (q) to zero: *i.e.*, for $\bar{B}_s \to K^0\omega$, $S_K^{(s)} = P_{\mathrm{EW},K}^{(s)} = 0$, and for $\bar{B}_s \to K^0\phi$, $C_K^{(q)} = S_K^{(q)} = P_K^{(q)} = \cdots = 0$.

$\bar{B}_s \to PV$	factor	$T_{P\ [V]}^{(\zeta)}$	$C_{P\ [V]}^{(\zeta)}$	$S_{P\ [V]}^{(\zeta)}$	$P_{P\ [V]}^{(\zeta)}$	$P_{\mathrm{EW},\ P\ [V]}^{(\zeta)}$	$P_{\mathrm{EW},\ P\ [V]}^{C,\ (\zeta)}$
$\bar{B}_s \to \pi^- K^{*+}$	1	0	0	0	0	0	0
		[1]	[0]	[0]	[1]	[0]	$[\frac{2}{3}]$
$\bar{B}_s \to \pi^0 K^{*0}$	$\frac{1}{\sqrt{2}}$	0	0	0	0	0	0
		[0]	[1]	[0]	$[-1]$	[1]	$[\frac{1}{3}]$
$\bar{B}_s \to \eta^{(\prime)} K^{*0}$	$\frac{1}{\sqrt{2}}$	0	0	0	$\sqrt{2}(s)$	0	$-\frac{\sqrt{2}}{3}(s)$
		[0]	$[1(q) + \sqrt{2}(c)]$	$[2(q) + \sqrt{2}(s) + \sqrt{2}(c)]$	$[1(q)]$	$[\frac{1}{3}(q) - \frac{\sqrt{2}}{3}(s)]$	$[-\frac{1}{3}(q)]$
$\bar{B}_s \to K^+ \rho^-$	1	1	0	0	1	0	$\frac{2}{3}$
		[0]	[0]	[0]	[0]	[0]	[0]
$\bar{B}_s \to K^0 \rho^0$	$\frac{1}{\sqrt{2}}$	0	1	0	-1	1	$\frac{1}{3}$
		[0]	[0]	[0]	[0]	[0]	[0]
$\bar{B}_s \to K^0\ \omega/\phi$	$\frac{1}{\sqrt{2}}$	0	$1(q)$	$2(q) + \sqrt{2}(s)$	$1(q)$	$\frac{1}{3}(q) - \frac{\sqrt{2}}{3}(s)$	$-\frac{1}{3}(q)$
		[0]	[0]	[0]	$[\sqrt{2}(s)]$	[0]	$[-\frac{\sqrt{2}}{3}(s)]$

TABLE XX: (*Continued from Table XIX*) Weak annihilation contributions. When ideal mixing for ω and ϕ is assumed, the same rules as used in *Table XIX* are applied.

$\bar{B}_s \to PV$	factor	$E^{(\zeta)}_{P\ [V]}$	$A^{(\zeta)}_{P\ [V]}$	$PE^{(\zeta)}_{P\ [V]}$	$PA^{(\zeta)}_{P\ [V]}$	$PE^{(\zeta)}_{\mathrm{EW},\ P\ [V]}$	$PA^{(\zeta)}_{\mathrm{EW},\ P\ [V]}$
$\bar{B}_s \to \pi^- K^{*+}$	1	0	0	0	0	0	0
		[0]	[0]	[1]	[0]	$[-\frac{1}{3}]$	[0]
$\bar{B}_s \to \pi^0 K^{*0}$	$\frac{1}{\sqrt{2}}$	0	0	0	0	0	0
		[0]	[0]	$[-1]$	[0]	$[\frac{1}{3}]$	[0]
$\bar{B}_s \to \eta^{(\prime)} K^{*0}$	$\frac{1}{\sqrt{2}}$	0	0	$\sqrt{2}(s)$	0	$-\frac{\sqrt{2}}{3}(s)$	0
		[0]	[0]	$[1(q)]$	[0]	$[-\frac{1}{3}(q)]$	[0]
$\bar{B}_s \to K^+ \rho^-$	1	0	0	1	0	$-\frac{1}{3}$	0
		[0]	[0]	[0]	[0]	[0]	[0]
$\bar{B}_s \to K^0 \rho^0$	$\frac{1}{\sqrt{2}}$	0	0	-1	0	$\frac{1}{3}$	0
		[0]	[0]	[0]	[0]	[0]	[0]
$\bar{B}_s \to K^0\ \omega/\phi$	$\frac{1}{\sqrt{2}}$	0	0	$1(q)$	0	$-\frac{1}{3}(q)$	0
		[0]	[0]	$[\sqrt{2}(s)]$	[0]	$[-\frac{\sqrt{2}}{3}(s)]$	[0]

TABLE XXI: (*Continued from Table XX*) Singlet weak annihilation contributions. When ideal mixing for ω and ϕ is assumed, the same rules as used in *Table XIX* are applied.

$\bar{B}_s \to PV$	factor	$SE^{(\zeta)}_{P\ [V]}$	$SA^{(\zeta)}_{P\ [V]}$	$SPE^{(\zeta)}_{P\ [V]}$	$SPA^{(\zeta)}_{P\ [V]}$	$SPE^{(\zeta)}_{\mathrm{EW},\ P\ [V]}$	$SPA^{(\zeta)}_{\mathrm{EW},\ P\ [V]}$
$\bar{B}_s \to \eta^{(\prime)} K^{*0}$	$\frac{1}{\sqrt{2}}$	0	0	0	0	0	0
		[0]	[0]	$[2(q)+\sqrt{2}(s)]$	[0]	$[-\frac{2}{3}(q)-\frac{\sqrt{2}}{3}(s)]$	[0]
$\bar{B}_s \to K^0\ \omega/\phi$	$\frac{1}{\sqrt{2}}$	0	0	$2(q)+\sqrt{2}(s)$	0	$-\frac{2}{3}(q)-\frac{\sqrt{2}}{3}(s)$	0
		[0]	[0]	[0]	[0]	[0]	[0]

TABLE XXII: Coefficients of $\mathrm{SU(3)_F}$ amplitudes in $\bar{B}_s \to PV$ ($|\Delta S| = 1$). When ideal mixing for ω and ϕ is assumed, i) for $\bar{B}_s \to \pi^0\omega$ ($\pi^0\phi$), set the coefficients of $\mathrm{SU(3)_F}$ amplitudes with the subscript π and the superscript $\zeta = s$ (q) to zero: *i.e.*, for $\bar{B}_s \to \pi^0\omega$, $SE'^{(s)}_{\pi} = SPA'^{(s)}_{\mathrm{EW},\pi} = 0$ [See *Tabel XXIV.*], and for $\bar{B}_s \to \pi^0\phi$, $E'^{(q)}_{\pi} = PA'^{(q)}_{\pi} = \cdots = 0$ [See *Tabel XXIII.*], and ii) for $\bar{B}_s \to \eta^{(\prime)}\omega$ [$\eta^{(\prime)}\phi$], set the coefficients of $\mathrm{SU(3)_F}$ amplitudes with the superscript $\zeta = (s,s)$ or (q,s) [(s,q) or (q,q)] to zero: *i.e.*, for $\bar{B}_s \to \eta^{(\prime)}\omega$, $C'^{(q,s)}_{\omega} = S'^{(s,s)}_{\eta^{(\prime)}} = S'^{(q,s)}_{\omega} = S'^{(s,s)}_{\omega} = \cdots = 0$, and for $\bar{B}_s \to \eta^{(\prime)}\phi$, $C'^{(s,q)}_{\eta^{(\prime)}} = S'^{(s,q)}_{\eta^{(\prime)}} = P'^{(s,q)}_{\mathrm{EW},\eta^{(\prime)}} = 0$.

$\bar{B}_s \to PV$	factor	$T'^{(\zeta)}_{P\ [V]}$	$C'^{(\zeta)}_{P\ [V]}$	$S'^{(\zeta)}_{P\ [V]}$	$P'^{(\zeta)}_{P\ [V]}$	$P'^{(\zeta)}_{\mathrm{EW},\ P\ [V]}$	$P^{C\prime,\ (\zeta)}_{\mathrm{EW},\ P\ [V]}$
$\bar{B}_s \to \pi^+\rho^-$	1	0	0	0	0	0	0
		[0]	[0]	[0]	[0]	[0]	[0]
$\bar{B}_s \to \pi^-\rho^+$	1	0	0	0	0	0	0
		[0]	[0]	[0]	[0]	[0]	[0]
$\bar{B}_s \to \pi^0\rho^0$	$\frac{1}{2}$	0	0	0	0	0	0
		[0]	[0]	[0]	[0]	[0]	[0]
$\bar{B}_s \to \bar{K}^0 K^{*0}$	1	0	0	0	0	0	0
		[0]	[0]	[0]	[1]	[0]	$[-\frac{1}{3}]$
$\bar{B}_s \to K^0 \bar{K}^{*0}$	1	0	0	0	1	0	$-\frac{1}{3}$
		[0]	[0]	[0]	[0]	[0]	[0]
$\bar{B}_s \to K^- K^{*+}$	1	0	0	0	0	0	0
		[1]	[0]	[0]	[1]	[0]	$[\frac{2}{3}]$
$\bar{B}_s \to K^+ K^{*-}$	1	1	0	0	1	0	$\frac{2}{3}$
		[0]	[0]	[0]	[0]	[0]	[0]
$\bar{B}_s \to \pi^0\ \omega/\phi$	$\frac{1}{2}$	0	0	0	0	0	0
		[0]	$[\sqrt{2}(s)]$	[0]	[0]	$[\sqrt{2}(s)]$	[0]
$\bar{B}_s \to \eta^{(\prime)}\rho^0$	$\frac{1}{2}$	0	$\sqrt{2}(s)$	0	0	$\sqrt{2}(s)$	0
		[0]	[0]	[0]	[0]	[0]	[0]
$\bar{B}_s \to \eta^{(\prime)}\ \omega/\phi$	$\frac{1}{2}$	0	$\sqrt{2}(s,q)$	$2\sqrt{2}(s,q) + 2(s,s)$	$2(s,s)$	$\frac{\sqrt{2}}{3}(s,q)$ $-\frac{2}{3}(s,s)$	$-\frac{2}{3}(s,s)$
		[0]	$[\sqrt{2}(q,s)$ $+2(c,s)]$	$[2\sqrt{2}(q,s) + 2(s,s)$ $+2(c,s)]$	$[2(s,s)]$	$[\frac{\sqrt{2}}{3}(q,s)$ $-\frac{2}{3}(s,s)]$	$[-\frac{2}{3}(s,s)]$

TABLE XXIII: (*Continued from Table XXII*) Weak annihilation contributions. When ideal mixing for ω and ϕ is assumed, the same rules as used in *Table XXII* are applied.

$\bar{B}_s \to PV$	factor	$E'^{(\zeta)}_{P\ [V]}$	$A'^{(\zeta)}_{P\ [V]}$	$PE'^{(\zeta)}_{P\ [V]}$	$PA'^{(\zeta)}_{P\ [V]}$	$PE'^{(\zeta)}_{\mathrm{EW},\ P\ [V]}$	$PA'^{(\zeta)}_{\mathrm{EW},\ P\ [V]}$
$\bar{B}_s \to \pi^+\rho^-$	1	0	0	0	1	0	$-\frac{1}{3}$
		[1]	[0]	[0]	[1]	[0]	$[\frac{2}{3}]$
$\bar{B}_s \to \pi^-\rho^+$	1	1	0	0	1	0	$\frac{2}{3}$
		[0]	[0]	[0]	[1]	[0]	$[-\frac{1}{3}]$
$\bar{B}_s \to \pi^0\rho^0$	$\frac{1}{2}$	1	0	0	2	0	$\frac{1}{3}$
		[1]	[0]	[0]	[2]	[0]	$[\frac{1}{3}]$
$\bar{B}_s \to \bar{K}^0 K^{*0}$	1	0	0	0	1	0	$-\frac{1}{3}$
		[0]	[0]	[1]	[1]	$[-\frac{1}{3}]$	$[-\frac{1}{3}]$
$\bar{B}_s \to K^0 \bar{K}^{*0}$	1	0	0	1	1	$-\frac{1}{3}$	$-\frac{1}{3}$
		[0]	[0]	[0]	[1]	[0]	$[-\frac{1}{3}]$
$\bar{B}_s \to K^- K^{*+}$	1	1	0	0	1	0	$\frac{2}{3}$
		[0]	[0]	[1]	[1]	$[-\frac{1}{3}]$	$[-\frac{1}{3}]$
$\bar{B}_s \to K^+ K^{*-}$	1	0	0	1	1	$-\frac{1}{3}$	$-\frac{1}{3}$
		[1]	[0]	[0]	[1]	[0]	$[\frac{2}{3}]$
$\bar{B}_s \to \pi^0\ \omega/\phi$	$\frac{1}{2}$	$1(q)$	0	0	0	0	$1(q)$
		$[1(q)]$	[0]	[0]	[0]	[0]	$[1(q)]$
$\bar{B}_s \to \eta^{(\prime)}\rho^0$	$\frac{1}{2}$	$1(q)$	0	0	0	0	$1(q)$
		$[1(q)]$	[0]	[0]	[0]	[0]	$[1(q)]$
$\bar{B}_s \to \eta^{(\prime)}\ \omega/\phi$	$\frac{1}{2}$	$1(q,q)$	0	$2(s,s)$	$2(q,q)$	$-\frac{2}{3}(s,s)$	$\frac{1}{3}(q,q)$
					$+2(s,s)$		$-\frac{2}{3}(s,s)$
		$[1(q,q)]$	0	$[2(s,s)]$	$[2(q,q)$	$[-\frac{2}{3}(s,s)]$	$[\frac{1}{3}(q,q)$
					$+2(s,s)]$		$-\frac{2}{3}(s,s)]$

TABLE XXIV: (*Continued from Table XXIII*) Singlet weak annihilation contributions. When ideal mixing for ω and ϕ is assumed, the same rules as used in *Table XXII* are applied.

$\bar{B}_s \to PV$	factor	$SE'^{(\zeta)}_{P\ [V]}$	$SA'^{(\zeta)}_{P\ [V]}$	$SPE'^{(\zeta)}_{P\ [V]}$	$SPA'^{(\zeta)}_{P\ [V]}$	$SPE'^{(\zeta)}_{\mathrm{EW},\ P\ [V]}$	$SPA'^{(\zeta)}_{\mathrm{EW},\ P\ [V]}$
$\bar{B}_s \to \pi^0\ \omega/\phi$	$\frac{1}{2}$	$2(q)+\sqrt{2}(s)$	0	0	0	0	$2(q)+\sqrt{2}(s)$
		$[0]$	$[0]$	$[0]$	$[0]$	$[0]$	$[0]$
$\bar{B}_s \to \eta^{(\prime)}\rho^0$	$\frac{1}{2}$	0	0	0	0	0	0
		$[2(q)+\sqrt{2}(s)]$	$[0]$	$[0]$	$[0]$	$[0]$	$[2(q)+\sqrt{2}(s)]$
$\bar{B}_s \to \eta^{(\prime)}\ \omega/\phi$	$\frac{1}{2}$	$2(q,q)$	0	$2\sqrt{2}(s,q)$	$4(q,q)+2\sqrt{2}(q,s)$	$-\frac{2\sqrt{2}}{3}(s,q)$	$\frac{2}{3}(q,q)+\frac{\sqrt{2}}{3}(q,s)$
		$+\sqrt{2}(q,s)$		$+2(s,s)$	$+2\sqrt{2}(s,q)+2(s,s)$	$-\frac{2}{3}(s,s)$	$-\frac{2\sqrt{2}}{3}(s,q)-\frac{2}{3}(s,s)$
		$[2(q,q)$	$[0]$	$[2\sqrt{2}(q,s)$	$[4(q,q)+2\sqrt{2}(s,q)$	$[-\frac{2\sqrt{2}}{3}(q,s)$	$[\frac{2}{3}(q,q)+\frac{\sqrt{2}}{3}(s,q)$
		$+\sqrt{2}(s,q)]$		$+2(s,s)]$	$+2\sqrt{2}(s,q)+2(s,s)]$	$-\frac{2}{3}(s,s)]$	$-\frac{2\sqrt{2}}{3}(q,s)-\frac{2}{3}(s,s)]$

TABLE XXV: Numerical values of the $\mathrm{SU(3)_F}$ amplitudes of $\bar{B}_{u,d} \to P_1P_2$ decays with $\Delta S = 0$ and $|\Delta S| = 1$ calculated in QCD factorization. The magnitude (in units of 10^{-9} GeV) and strong phase (in degrees) of each $\mathrm{SU(3)_F}$ amplitude are shown in order within the parenthesis : e.g., for the tree amplitude $T_P \equiv |T_P|\ e^{i(\delta_P+\theta_P)}$ with δ_P and θ_P being the strong and weak phases, respectively, its magnitude and strong phase are shown as $(|T_P|,\ \delta_P)$.

$\Delta S = 0$	Numerical values	$\lvert\Delta S\rvert = 1$	Numerical values
T_P	$(24.52,\ 0.9^\circ)$	T'_P	$(6.90,\ 0.9^\circ)$
C_P	$(15.47,\ -54.8^\circ)$	C'_P	$(4.48,\ -56.6^\circ)$
$S_P^{(q)}$	$(0.87,\ 159.1^\circ)$	$S_P^{\prime(q)}$	$(4.11,\ 150.3^\circ)$
$S_P^{(s)}$	$(0.89,\ 159.1^\circ)$	$S_P^{\prime(s)}$	$(4.21,\ 150.3^\circ)$
$S_P^{(c)}$	$(0.02,\ 159.1^\circ)$	$S_P^{\prime(c)}$	$(0.09,\ 150.3^\circ)$
P_P	$(5.59,\ -157.7^\circ)$	P'_P	$(34.25,\ -157.4^\circ)$
$P_{\mathrm{EW},\ P}$	$(0.82,\ -178.9^\circ)$	$P'_{\mathrm{EW},\ P}$	$(5.48,\ -178.9^\circ)$
$P^C_{\mathrm{EW},\ P}$	$(0.17,\ 163.9^\circ)$	$P^{C\prime}_{\mathrm{EW},\ P}$	$(1.05,\ 163.1^\circ)$
E_P	$(1.96,\ 52.7^\circ)$	E'_P	$(0.54,\ 52.9^\circ)$
A_P	$(0.61,\ -127.3^\circ)$	A'_P	$(0.17,\ -127.1^\circ)$
PE_P	$(3.79,\ -146.2^\circ)$	PE'_P	$(21.19\ ,\ -146.2^\circ)$
PA_P	$(0.61,\ -127.3^\circ)$	PA'_P	$(3.46,\ -127.1^\circ)$
$PE_{\mathrm{EW},\ P}$	$(0.02,\ -34.1^\circ)$	$PE'_{\mathrm{EW},\ P}$	$(0.13,\ -36.1^\circ)$
$PA_{\mathrm{EW},\ P}$	$(0.03,\ 52.7^\circ)$	$PA'_{\mathrm{EW},\ P}$	$(0.15,\ 52.9^\circ)$

TABLE XXVI: Same as Table XXV except for $\bar{B}_{u,d} \to PV$ decays : e.g., for the tree amplitudes $(T_P\ ;\ T_V)$ where $T_{P,V} \equiv |T_{P,V}|\ e^{i(\delta_{P,V}+\theta_{P,V})}$ with $\delta_{P,V}$ and $\theta_{P,V}$ being the strong and weak phases, respectively, their magnitudes (in units of 10^{-9} GeV) and strong phases (in degrees) are shown as $(|T_P|,\ \delta_P\ ;\ |T_V|,\ \delta_V)$.

$\Delta S = 0$	Numerical values	$\lvert\Delta S\rvert = 1$	Numerical values
$(\ T_P\ ;\ T_V\ )$	$(\ 40.82,\ 0.8^\circ\ ;\ 30.16,\ 0.8^\circ)$	$(\ T'_P\ ;\ T'_V\ )$	$(\ 9.63,\ 0.8^\circ\ ;\ 8.54,\ 0.8^\circ)$
$(\ C_P\ ;\ C_V\ )$	$(\ 12.30,\ -16.0^\circ\ ;\ 11.84,\ -51.7^\circ)$	$(\ C'_P\ ;\ C'_V\ )$	$(\ 3.38,\ -19.0^\circ\ ;\ 2.79,\ -55.4^\circ)$
$(\ S_P^{(q)}\ ;\ S_V^{(q)}\ )$	$(\ 0.50,\ -4.7^\circ\ ;\ 0.79,\ 151.5^\circ)$	$(\ S_P^{\prime(q)}\ ;\ S_V^{\prime(q)}\ )$	$(\ 2.75,\ -5.6^\circ\ ;\ 3.04,\ 134.2^\circ)$
$(\ S_P^{(s)}\ ;\ S_V^{(s)}\ )$	$(\ 0.59,\ -4.6^\circ\ ;\ 0.81,\ 151.5^\circ)$	$(\ S_P^{\prime(s)}\ ;\ S_V^{\prime(s)}\ )$	$(\ 3.22,\ -5.5^\circ\ ;\ 3.11,\ 134.2^\circ)$
$(\ S_P^{(c)}\ ;\ S_V^{(c)}\ )$	$(\ -\ ;\ 0.02,\ 151.5^\circ)$	$(\ S_P^{\prime(c)}\ ;\ S_V^{\prime(c)}\ )$	$(\ -\ ;\ 0.07,\ 134.2^\circ)$
$(\ P_P\ ;\ P_V\ )$	$(\ 3.04,\ -144.7^\circ\ ;\ 3.12,\ 8.4^\circ)$	$(\ P'_P\ ;\ P'_V\ )$	$(\ 17.99,\ -144.4^\circ\ ;\ 17.02,\ 7.9^\circ)$
$(\ P_{\rm EW,\ P}\ ;\ P_{\rm EW,\ V})$	$(\ 1.41,\ -179.4^\circ\ ;\ 1.01,\ -178.9^\circ)$	$(\ P'_{\rm EW,\ P}\ ;\ P'_{\rm EW,\ V})$	$(\ 9.39,\ -179.4^\circ\ ;\ 6.00,\ -178.9^\circ)$
$(\ P^C_{\rm EW,\ P}\ ;\ P^C_{\rm EW,\ V})$	$(\ 0.38,\ 165.0^\circ\ ;\ 0.34,\ 164.7^\circ)$	$(\ P^{C\prime}_{\rm EW,\ P}\ ;\ P^{C\prime}_{\rm EW,\ V})$	$(\ 1.76,\ 165.1^\circ\ ;\ 1.87,\ 160.6^\circ)$
$(\ E_P\ ;\ E_V\ )$	$(\ 2.46,\ 70.1^\circ\ ;\ 2.29,\ 38.9^\circ)$	$(\ E'_P\ ;\ E'_V\ )$	$(\ 0.60,\ 69.4^\circ\ ;\ 0.64,\ 39.2^\circ)$
$(\ A_P\ ;\ A_V\ )$	$(\ 0.77,\ -109.9^\circ\ ;\ 0.72,\ -141.1^\circ)$	$(\ A'_P\ ;\ A'_V\ )$	$(\ 0.19,\ -110.6^\circ\ ;\ 0.20,\ -140.8^\circ)$
$(\ PE_P\ ;\ PE_V\ )$	$(\ 3.82,\ -123.6^\circ\ ;\ 3.83,\ 5.3^\circ)$	$(\ PE'_P\ ;\ PE'_V\ )$	$(\ 19.83,\ -124.2^\circ\ ;\ 21.20,\ 5.0^\circ)$
$(\ PA_P\ ;\ PA_V\ )$	$(\ 0.12,\ 70.1^\circ\ ;\ 0.11,\ 38.9^\circ)$	$(\ PA'_P\ ;\ PA'_V\ )$	$(\ 0.61,\ 69.4^\circ\ ;\ 0.66,\ 39.2^\circ)$
$(\ PE_{\rm EW,\ P}\ ;\ PE_{\rm EW,\ V})$	$(\ 0.02,\ -57.8^\circ\ ;\ 0.14,\ -157.3^\circ)$	$(\ PE'_{\rm EW,\ P}\ ;\ PE'_{\rm EW,\ V})$	$(\ 0.10,\ -50.7^\circ\ ;\ 0.77,\ -157.0^\circ)$
$(\ PA_{\rm EW,\ P}\ ;\ PA_{\rm EW,\ V})$	$(\ 0.02,\ 70.1^\circ\ ;\ 0.02,\ 38.9^\circ)$	$(\ PA'_{\rm EW,\ P}\ ;\ PA'_{\rm EW,\ V})$	$(\ 0.08,\ 69.4^\circ\ ;\ 0.09,\ 39.2^\circ)$

TABLE XXVII: Same as Table XXV except for $\bar{B}_s \to P_1 P_2$ decays.

$\Delta S = 0$	Numerical values	$\lvert\Delta S\rvert = 1$	Numerical values
T_P	$(23.54,\ 0.9°)$	T'_P	$(6.61,\ 0.8°)$
C_P	$(19.57,\ -51.6°)$	C'_P	$(5.72,\ -50.5°)$
$S_P^{(q)}$	$(1.31,\ 166.6°)$	$S_P^{\prime(s,q)}$	$(3.53,\ 162.5°)$
$S_P^{(s)}$	$(1.35,\ 166.6°)$	$S_P^{\prime(s,s)}$	$(3.62,\ 162.5°)$
$S_P^{(c)}$	$(0.03,\ 166.6°)$	$S_P^{\prime(s,c)}$	$(0.08,\ 162.5°)$
P_P	$(5.64,\ -158.1°)$	P'_P	$(34.69,\ -157.9°)$
$P_{\rm EW,\ P}$	$(0.78,\ -178.9°)$	$P'_{\rm EW,\ P}$	$(4.46,\ -178.8°)$
$P^C_{\rm EW,\ P}$	$(0.25,\ 170.0°)$	$P^{C\prime}_{\rm EW,\ P}$	$(1.58,\ 171.0°)$
E_P	$(2.35,\ 51.2°)$	E'_P	$(0.65,\ 51.4°)$
A_P	$(0.74,\ -128.8°)$	A'_P	$(0.20,\ -128.6°)$
PE_P	$(4.31,\ -149.1°)$	PE'_P	$(24.12,\ -149.1°)$
PA_P	$(0.74,\ -128.8°)$	PA'_P	$(4.18,\ -128.6°)$
$PE_{\rm EW,\ P}$	$(0.03,\ -46.2°)$	$PE'_{\rm EW,\ P}$	$(0.15,\ -48.4°)$
$PA_{\rm EW,\ P}$	$(0.03,\ 51.2°)$	$PA'_{\rm EW,\ P}$	$(0.18,\ 51.4°)$

TABLE XXVIII: Same as Table XXVI except for $\bar{B}_s \to PV$ decays.

$\Delta S = 0$	Numerical values	$\lvert\Delta S\rvert = 1$	Numerical values
$(\ T_P\ ;\ T_V\ )$	$(\ 39.33,\ 0.9°\ ;\ 30.59,\ 0.8°)$	$(\ T'_P\ ;\ T'_V\ )$	$(\ 9.28,\ 0.9°\ ;\ 8.60,\ 0.9°)$
$(\ C_P\ ;\ C_V\ )$	$(\ 15.49,\ -12.5°\ ;\ 12.90,\ -50.6°)$	$(\ C'_P\ ;\ C'_V\ )$	$(\ 3.59,\ -13.0°\ ;\ 3.82,\ -50.7°)$
$(\ S_P^{(q)}\ ;\ S_V^{(q)}\ )$	$(\ 0.64,\ -3.6°\ ;\ 0.91,\ 155.3°)$	$(\ S_P^{\prime(s,q)}\ ;\ S_V^{\prime(q,s)}\ )$	$(\ 1.90,\ -4.3°\ ;\ 4.56,\ 155.1°)$
$(\ S_P^{(s)}\ ;\ S_V^{(s)}\ )$	$(\ 0.76,\ -3.6°\ ;\ 0.94,\ 155.3°)$	$(\ S_P^{\prime(s,s)}\ ;\ S_V^{\prime(s,s)}\ )$	$(\ 2.24,\ -4.2°\ ;\ 4.68,\ 155.1°)$
$(\ S_P^{(c)}\ ;S_V^{(c)}\ )$	$(\ -\ ;\ 0.02,\ 155.3°)$	$(\ S_P^{\prime(s,c)}\ ;\ S_V^{\prime(c,s)}\ )$	$(\ -\ ;\ 0.10,\ 155.1°)$
$(\ P_P\ ;\ P_V\ )$	$(\ 2.82,\ -142.7°\ ;\ 3.51,\ 7.7°\ )$	$(\ P'_P\ ;\ P'_V\ )$	$(\ 16.71,\ -142.1°\ ;\ 19.83,\ 6.7°)$
$(\ P_{\rm EW,\ P}\ ;\ P_{\rm EW,\ V}\ )$	$(\ 1.38,\ -179.4°\ ;\ 1.03,\ -178.9°)$	$(\ P'_{\rm EW,\ P}\ ;\ P'_{\rm EW,\ V}\ )$	$(\ 6.61,\ -179.4°\ ;\ 5.89,\ -178.9°)$
$(\ P^C_{\rm EW,\ P}\ ;\ P^C_{\rm EW,\ V}\ )$	$(\ 0.48,\ 168.6°\ ;\ 0.36,\ 164.9°)$	$(\ P^{C\prime}_{\rm EW,\ P}\ ;\ P^{C\prime}_{\rm EW,\ V}\ )$	$(\ 2.30,\ 168.2°\ ;\ 2.10,\ 164.6°)$
$(\ E_P\ ;\ E_V\ )$	$(\ 3.24,\ 70.5°\ ;\ 2.44,\ 45.0°)$	$(\ E'_P\ ;\ E'_V\ )$	$(\ 0.79,\ 69.8°\ ;\ 0.68,\ 45.4°)$
$(\ A_P\ ;\ A_V\ )$	$(\ 1.01,\ -109.5°\ ;\ 0.76,\ -135.0°)$	$(\ A'_P\ ;\ A'_V\ )$	$(\ 0.25,\ -110.2°\ ;\ 0.21,\ -134.6°)$
$(\ PE_P\ ;\ PE_V\ )$	$(\ 4.87,\ -123.4°\ ;\ 4.01,\ 16.3°)$	$(\ PE'_P\ ;\ PE'_V\ )$	$(\ 25.33,\ -124.0°\ ;\ 22.29,\ 16.1°)$
$(\ PA_P\ ;\ PA_V\ )$	$(\ 0.16,\ 70.5°\ ;\ 0.12,\ 45.0°)$	$(\ PA'_P\ ;\ PA'_V\ )$	$(\ 0.81,\ 69.8°\ ;\ 0.70,\ 45.4°)$
$(\ PE_{\rm EW,\ P}\ ;\ PE_{\rm EW,\ V}\ )$	$(\ 0.03,\ -63.1°\ ;\ 0.15,\ -148.7°)$	$(\ PE'_{\rm EW,\ P}\ ;\ PE'_{\rm EW,\ V}\ )$	$(\ 0.13,\ -56.1°\ ;\ 0.82,\ -148.4°)$
$(\ PA_{\rm EW,\ P}\ ;\ PA_{\rm EW,\ V}\ )$	$(\ 0.02,\ 70.5°\ ;\ 0.02,\ 45.0°)$	$(\ PA'_{\rm EW,\ P}\ ;\ PA'_{\rm EW,\ V}\ )$	$(\ 0.11,\ 69.8°\ ;\ 0.09,\ 45.4°)$

[1] A. Ali and C. Greub, Phys. Rev. D **57**, 2996 (1998).

[2] Y.H. Chen, H.Y. Cheng, B. Tseng and K.C. Yang, Phys. Rev. D **60**, 094014 (1999).

[3] M. Beneke, G. Buchalla, M. Neubert and C.T. Sachrajda, Phys. Rev. Lett. **83**, 1914 (1999); Nucl. Phys. B **591**, 313 (2000).

[4] Y.Y. Keum, H.-n. Li and A.I. Sanda, Phys. Rev. D **63**, 054008 (2001).

[5] C.W. Bauer, D. Pirjol, I.Z. Rothstein and I.W. Stewart, Phys. Rev. D **70**, 054015 (2004).

[6] L. L. Chau Wang, p. 419-431 in AIP Conference Proceedings 72 (1980), Weak Interactions as Probes of Unification (edited by G.B. Collins, L.N. Chang and J.R. Ficenec), and p.1218-1232 in Proceedings of the 1980 Guangzhou Conference on Theoretical Particle Physics (Science Press, Beijing, China, 1980, distributed by Van Nostrand Reinhold company); L. L. Chau, Phys. Rep. **95**, 1 (1983).

[7] L.L. Chau and H.Y. Cheng, Phys. Rev. Lett. **56**, 1655 (1986).

[8] L.L. Chau and H.Y. Cheng, Phys. Rev. D **36**, 137 (1987); Phys. Lett. B **222**, 285 (1989).

[9] L.L. Chau, H.Y. Cheng, W. K. Sze, H. Yao, and B. Tseng, Phys. Rev. D **43**, 2176-2192 (1991); Phys. Rev. D **58**, 019902(E) (1998).

[10] C. W. Chiang, M. Gronau, Z. Luo, J. L. Rosner and D. A. Suprun, Phys. Rev. D **69**, 034001 (2004) [arXiv:hep-ph/0307395].

[11] C.W. Chiang, M. Gronau, J.L. Rosner and D. Suprun, Phys. Rev. D **70**, 034020 (2004).

[12] C. W. Chiang, Y.F. Zhou, JHEP **0612**, 027 (2006) [hep-ph/0609128].

[13] C. W. Chiang, Y. F. Zhou, JHEP **0903**, 055 (2009) [arXiv:0809.0841 [hep-ph]].

[14] D. Zeppenfeld, Z. Phys. C **8**, 77 (1981).

[15] M. Gronau, O. F. Hernandez, D. London, J. L. Rosner, Phys. Rev. D **50**, 4529 (1994) [hep-ph/9404283]; Phys. Rev. D **52**, 6356 (1995) [hep-ph/9504326]; *ibid.*, 6374 (1995) [hep-ph/9504327]; A. S. Dighe, M. Gronau and J. L. Rosner, Phys. Lett. B **367**, 357 (1996) [Erratum-ibid. B **377**, 325 (1996)] [arXiv:hep-ph/9509428]; Phys. Rev. D **57**, 1783 (1998) [hep-ph/9709223].

[16] S. Oh, Phys. Rev. D **60**, 034006 (1999) [arXiv:hep-ph/9812530].

[17] N. G. Deshpande, X. -G. He, J. -Q. Shi, Phys. Rev. D **62**, 034018 (2000) [hep-ph/0002260]; M. A. Dariescu, N. G. Deshpande, X. -G. He, G. Valencia, Phys. Lett. B **557**, 60 (2003)

[hep-ph/0212333].

[18] X.Y. Li and S.F. Tuan, DESY Report No. 83-078 (unpublished); X.Y. Li, X.Q. Li, and P. Wang, Nuovo Ciemento **100A**, 693 (1988).

[19] L.L. Chau and H.Y. Cheng, Phys. Rev. D **39**, 2788 (1989); L.L. Chau, H.Y. Cheng, and T. Huang, Z. Phys. C **53**, 413 (1992).

[20] M. Beneke, G. Buchalla, M. Neubert and C. T. Sachrajda, Phys. Rev. Lett. **83**, 1914 (1999) [arXiv:hep-ph/9905312]; Nucl. Phys. B **591**, 313 (2000) [arXiv:hep-ph/0006124].

[21] M. Beneke and M. Neubert, Nucl. Phys. B **675**, 333 (2003) [arXiv:hep-ph/0308039].

[22] M. Beneke, J. Rohrer and D. Yang, Nucl. Phys. B **774**, 64 (2007) [arXiv:hep-ph/0612290].

[23] M. Wirbel, B. Stech, and M. Bauer, Z. Phys. C **29**, 637 (1985); M. Bauer, B. Stech and M. Wirbel, Z. Phys. C **34**, 103 (1987).

[24] H. Y. Cheng and C. K. Chua, Phys. Rev. D **80**, 114008 (2009) [arXiv:0909.5229 [hep-ph]]; *ibid.*, 114026 (2009) [arXiv:0910.5237 [hep-ph]].

[25] P. Ball and R. Zwicky, Phys. Rev. D **71**, 014015 (2005) [arXiv:hep-ph/0406232]; *ibid.*, 014029 (2005) [arXiv:hep-ph/0412079].

[26] H. Y. Cheng, C. K. Chua and C. W. Hwang, Phys. Rev. D **69**, 074025 (2004) [arXiv:hep-ph/0310359].

[27] T. Feldmann, P. Kroll and B. Stech, Phys. Rev. D **58**, 114006 (1998) [arXiv:hep-ph/9802409]; Phys. Lett. B **449**, 339 (1999) [arXiv:hep-ph/9812269].

[28] P. Ball, G. W. Jones and R. Zwicky, Phys. Rev. D **75**, 054004 (2007) [arXiv:hep-ph/0612081].

[29] H. Y. Cheng and C. K. Chua, Phys. Rev. D **80**, 074031 (2009) [arXiv:0908.3506 [hep-ph]].

[30] A. S. Dighe, M. Gronau, J. L. Rosner, Phys. Rev. Lett. **79**, 4333 (1997) [hep-ph/9707521]; C. W. Chiang and J. L. Rosner, Phys. Rev. D **65**, 074035 (2002) [Erratum-ibid. D **68**, 039902 (2003)] [arXiv:hep-ph/0112285]; H. K. Fu, X. G. He and Y. K. Hsiao, Phys. Rev. D **69**, 074002 (2004) [arXiv:hep-ph/0304242]; C. W. Chiang, M. Gronau and J. L. Rosner, Phys. Rev. D **68**, 074012 (2003) [arXiv:hep-ph/0306021].

[31] H.J. Lipkin, Phys. Lett. B **254**, 247 (1991); Phys. Lett. B **433**, 117 (1998).

[32] M. Beneke and M. Neubert, Nucl. Phys. B **651**, 225 (2003) [arXiv:hep-ph/0210085].